Commun Nonlinear Sci Numer Simulat 161 (2026) 110041

Contents lists available at ScienceDirect

Communications in Nonlinear Science and Numerical Simulation

journal homepage: www.elsevier.com/locate/cnsns

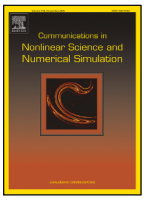

Research paper

Neural network-based adaptive fixed-time control for nonlinear systems with actuator faults, unmodeled dynamics, and input dead-zone

Mohamed Kharrat [a], Paolo Mercorelli [b,*]

[a] Mathematics Department, College of Science, Jouf University, Sakaka, Saudi Arabia
[b] Institute for Production Technology and Systems, Leuphana University of Lueneburg, 21335, Lueneburg, Germany

ARTICLE INFO

Keywords:
Nonlinear system
Actuator faults
Unmodeled dynamics
Dead-zone
Fixed-time stability

ABSTRACT

This work presents an adaptive fixed-time control scheme for nonstrict-feedback nonlinear systems, taking into account the presence of actuator faults, input dead-zone, unmodeled dynamics, and external disturbances. Radial basis function neural networks (RBFNNs) are employed to approximate the unknown nonlinearities, and a dynamic auxiliary signal is incorporated to handle the effects of unmodeled dynamics. By combining the backstepping design with Lyapunov stability theory, the proposed adaptive fixed-time controller guarantees that all closed-loop signals remain bounded and that the system output tracks the desired trajectory within a fixed duration. Importantly, the settling time is determined solely by the selected controller parameters and is independent of the initial system states. The proposed control approach is validated and its practicality is illustrated using both a numerical simulation and a pendulum system example.

1. Introduction

Industrial applications such as robotics, inverted pendulums, and stirred tank reactors frequently involve nonlinear dynamic systems, which are characterized by nonlinear ordinary differential equations [1]. IRecent progress in nonlinear system control has introduced a range of advanced strategies, such as sliding mode techniques, smart control approaches, and adaptive backstepping methods [2,3]. Among these strategies, the adaptive backstepping approach, characterized by its recursive Lyapunov-based scheme, has emerged as a pivotal control methodology for managing a diverse range of systems and processes [4]. The growing interest and demand for addressing nonlinear systems in recent years are primarily driven by the fact that most practical physical systems exhibit nonlinear characteristics, leading to significant popularity in research on adaptive backstepping control [5,6]. It should be emphasized that conventional methods rely on prior information or a linear representation of the structural uncertainties inherent in nonlinear systems. Nevertheless, this requirement presents challenges in many practical situations, as obtaining an exact nonlinear model of real-world systems is often difficult. With the advancement of intelligent control theory, the use of neural networks (NNs) or fuzzy logic systems (FLSs) has become common in controller design, leading to numerous important contributions [7–11]. For example, an adaptive control method for nonlinear systems with time delays under a nonstrict-feedback structure, employing neural networks, is presented in [12]. Additionally, an adaptive fuzzy control scheme has been developed for output-constrained nonstrict-feedback nonlinear systems with input delays, as reported in [13]. Moreover, a consensus control strategy using event-triggering has been proposed for nonlinear systems utilizing neural networks within a nonstrict-feedback framework, as described in [14].

* Corresponding author.
E-mail address: paolo.mercorelli@leuphana.de (P. Mercorelli).

https://doi.org/10.1016/j.cnsns.2026.110041
Received 26 April 2025; Received in revised form 28 January 2026; Accepted 13 April 2026
Available online 15 April 2026

The previously reported results often overlook the influences of unmodeled dynamics and external disturbances, which are commonly encountered in practical engineering systems [15]. Unmodeled dynamics present significant challenges due to external disturbances, measurement noise, and modeling inaccuracies, often leading to degraded system performance or even instability [16]. Consequently, addressing control challenges posed by nonlinear systems affected by unmodeled dynamics has received increasing attention, resulting in the development of various effective control strategies [17,18]. For example, dynamic auxiliary signals have been incorporated into control schemes to reduce the effects of unmodeled dynamics and improve overall system performance [19]. Observer-based fuzzy adaptive control methods have also been developed for nonlinear systems experiencing unmodeled dynamics and time delays [20], while adaptive control strategies for strict-feedback nonlinear systems have been designed to handle dynamic uncertainties and time delays [21]. Nevertheless, these methods typically assume fully operational actuators and do not account for possible actuator faults.

In real-world industrial systems, actuator faults are common and can significantly impair performance or even lead to severe instability [22,23]. To enhance system reliability and safety, fault-tolerant control strategies have been developed to handle actuator faults in nonlinear systems [24,25]. Illustrative examples include fuzzy output-feedback adaptive fault-tolerant control for systems with actuator faults [26], adaptive control for strict-feedback nonlinear systems with unknown control direction and actuator faults using neural networks combined with dynamic surface control [27], and fault-tolerant adaptive output-feedback control for switched nonlinear systems with unmodeled dynamics based on a small-gain approach [28]. However, these studies generally address either unmodeled dynamics or actuator faults separately, and do not tackle both issues concurrently within a single framework.

The dead-zone, a prominent non-smooth nonlinearity frequently observed in industrial devices such as valves and DC servo motors, can significantly degrade system performance if not properly handled [29]. Ignoring this nonlinearity may lead to reduced control accuracy, impaired performance, potential equipment damage, and even system instability. Therefore, incorporating the dead-zone into controller design is essential for achieving optimal system behavior [30]. Various adaptive control approaches, based on fuzzy logic or neural networks, have been proposed to tackle nonlinear systems affected by unknown dead-zone characteristics [31,32]. For instance, an event-triggered adaptive control scheme using fuzzy logic systems has been developed for nonlinear systems with dead-zone effects [33]. Likewise, an adaptive control strategy addressing nonlinear systems with dead-zone and time-varying state constraints has been introduced using an output-feedback approach [34]. Additionally, an adaptive control method integrating predefined performance objectives and observer-based implementation has been proposed for nonlinear systems subject to dead-zone nonlinearity [35].

Furthermore, the system performance discussed in all the aforementioned results is related to the behavior as time approaches infinity. However, from a practical standpoint, it is more aligned with requirements to achieve the control objective within a finite or fixed time [36]. Finite-time control offers better transient performance and robustness compared to traditional control methods, making it an area of significant interest with notable research contributions in recent years [37,38]. For example, an adaptive finite-time control method has been introduced to handle nonlinear systems with unmodeled dynamics [39]. In a similar vein, an adaptive fuzzy finite-time control strategy has been designed for stochastic nonlinear systems subject to actuator faults [40]. However, a drawback of finite-time control is its potential variability in settling time, which can limit its applicability based on the initial states [41]. In contrast, the emergence of fixed-time control methods provides a compelling alternative that overcomes the dependency on initial states for achieving fast convergence [42]. This characteristic is particularly advantageous for ensuring system stability within a fixed time. Notably, fixed-time stability has demonstrated excellent performance in numerous practical applications [43–45]. For example, an adaptive control problem for stochastic nonlinear pure-feedback systems has been addressed using fixed-time stability theory [46]. Moreover, FLSs have been used with a fixed-time adaptive control technique to address nonlinear strict-feedback switched systems [47]. Additionally, an adaptive control strategy has been devised to address actuator hysteresis and state constraints in nonlinear systems, incorporating fixed-time theory and fuzzy approximation capabilities [48].

Motivated by the aforementioned studies, this work focuses on the adaptive control of nonlinear systems using a fixed-time control framework. A systematic fixed-time adaptive control scheme is developed by combining the backstepping design with Lyapunov stability theory, guaranteeing that all closed-loop signals converge within a predetermined fixed time. The proposed method effectively tackles practical challenges such as unmodeled dynamics, actuator faults, input dead-zone, and external disturbances, which often compromise control performance in real-world nonlinear systems. The key contributions of this paper are outlined as follows:

(1) Compared with recent works [42–45], this study develops an adaptive fixed-time control framework for nonstrict-feedback nonlinear systems subject to unmodeled dynamics, actuator faults, input dead-zone, and external disturbances. Unlike existing approaches [22,23,31], which address actuator faults and input dead-zone separately, the proposed design simultaneously accounts for their coupled effects, thereby capturing more realistic actuator characteristics. To mitigate the adverse influence of unmodeled dynamics, a dynamic compensating signal is incorporated into the control law. Moreover, radial basis function neural networks (RBFNNs) are employed to approximate unknown nonlinear functions, effectively reducing modeling uncertainty and simplifying adaptive parameter adjustment.

(2) In contrast to finite-time control schemes [36,37], whose settling time depends on initial conditions, the proposed fixed-time adaptive controller ensures convergence within a preassigned time bound that is entirely independent of initial states. This property enhances the controller's predictability, reliability, and applicability to practical systems where initial conditions are uncertain or variable. By properly selecting design parameters, the proposed controller achieves improved tracking precision, reduced steady-state error, and superior robustness against disturbances and actuator nonlinearities compared with existing finite-time approaches.

(3) Extensive simulation studies and quantitative comparisons based on performance evaluation metrics are conducted to verify the effectiveness and advantages of the proposed control strategy. The obtained results confirm that the developed scheme guarantees fixed-time convergence and boundedness of all closed-loop signals, while exhibiting faster transient response, enhanced tracking accuracy, and improved fault-tolerant capability relative to existing methods.

The organization of this paper is as follows: Section 2 provides the problem formulation and relevant preliminaries. Section 3 details the design of the controller along with stability analysis. Section 4 illustrates simulation results that demonstrate the effectiveness of the proposed approach. Finally, Section 5 concludes the study.

2. Problem formulation and preliminaries

Consider the following nonstrict-feedback nonlinear systems subject to unmodeled dynamics, actuator faults, dead-zone, and external disturbances:

$$\begin{cases} \dot{z} = q(z, \chi), \\ \dot{\chi}_i = g_i(\bar{\chi}_i)\chi_{i+1} + f_i(\chi) + \phi_i(\chi, z, t) + d_i(t), \quad i = 1, 2, \dots, n-1, \\ \dot{\chi}_n = g_n(\bar{\chi}_n)u^f + f_n(\chi) + \phi_n(\chi, z, t) + d_n(t), \\ y = \chi_1, \end{cases} \tag{1}$$

where $\bar{\chi}_i = [\chi_1, \dots, \chi_i]^T \in \mathbb{R}^i$ for $i = 1, \dots, n$ and $\chi = [\chi_1, \dots, \chi_n]^T \in \mathbb{R}^n$ denote the system state vectors. Here, $u^f \in \mathbb{R}$ is the system input, $y \in \mathbb{R}$ is the system output, and $d_i(t)$ represents bounded external disturbances. The functions $f_i(\chi)$ and $g_i(\bar{\chi}_i)$ for $i = 1, \dots, n$ are unknown smooth nonlinear functions. To guarantee controllability of the system, it is assumed that $g_i(\bar{\chi}_i) \neq 0, \quad i = 1, 2, \dots, n$. $d_i(t)$ represents bounded external disturbances. $z \in \mathbb{R}^{n_0}$ symbolizes the unmeasurable portion of the state, z-dynamics in (1) symbolizes the unmodeled dynamics, and ϕ_i denotes system dynamic uncertainty. $\phi_i(.)$ and $z(.)$ in (1) are supposed to be Lipschitz functions. This paper adopts the actuator fault model expressed as [40]

$$u^f = K(t)u(v) + L(t) \tag{2}$$

where $0 < K(t) \leq 1$ is referred to as the actuator efficiency factor, which may vary with time either slowly or rapidly, $L(t)$ denotes an additional bias fault. The dead-zone characteristic, denoted as $u(v)$, is defined as follows [41]

$$u(v) = \begin{cases} m_r(v(t) - b_r) & \text{if } v(t) \geq b_r \\ 0 & \text{if } -b_l < v(t) < b_r \\ m_l(v(t) + b_l) & \text{if } v(t) \leq -b_l \end{cases} \tag{3}$$

where v is the control input, m_r and m_l represent the slopes of the dead zone, while b_r and b_l denote the breakpoints. Then (3) can be expressed as

$$u(v) = m(t)v + \beta(t) \tag{4}$$

with

$$m(t) = \begin{cases} m_l & \text{if } v \leq 0 \\ m_r & \text{if } v > 0 \end{cases} \tag{5}$$

and

$$\beta(t) = \begin{cases} -m_r b_r & \text{if } v \geq b_r \\ -m(t)v & \text{if } -b_l < v < b_r \\ m_l b_l & \text{if } v \leq -b_l \end{cases} \tag{6}$$

It is easy to know that

$$\begin{cases} \min(m_r, m_l) = \underline{m} \leq |m(t)| \leq \bar{m} = \max(m_r, m_l) \\ \min(m_r b_r, m_l b_l) = \underline{\beta} \leq |\beta(t)| \leq \bar{\beta} = \max(m_r b_r, m_l b_l). \end{cases} \tag{7}$$

Following the approach in [41], it is assumed that $\underline{m}$ and $\bar{m}$ are known.

The architecture of the control system is depicted in Fig. 1.

Remark 1. In contrast to the systems discussed in [46] and [47], which focus on pure-feedback or nonlinear systems, system (1) involves nonlinear functions $f_i(\cdot)$ that relate to the entire system states. As a result, system (1) is categorized as a nonstrict-feedback system. Designing controllers for nonstrict-feedback systems is important because these systems are commonly found in real-world applications like electromechanical systems, aircraft, mass-spring-damper systems, and robots [42].

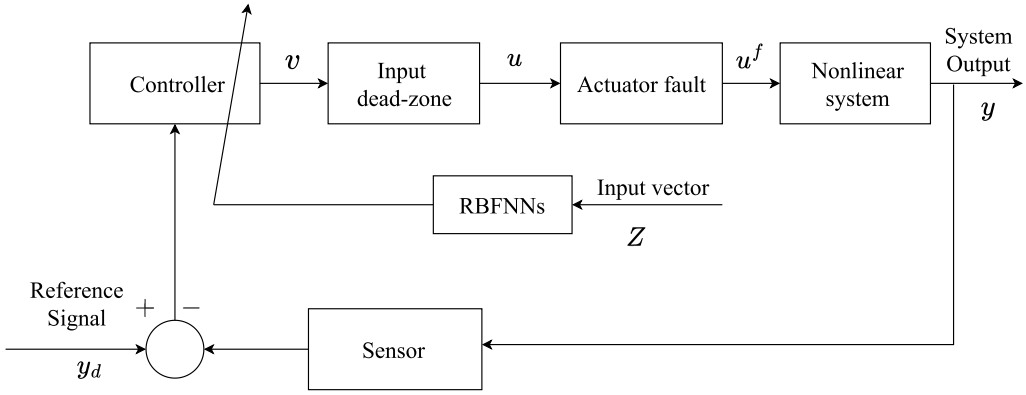

Fig. 1. Block diagram of control system.

The goal is to develop a fixed-time controller for the system (1) to ensure that:

(i) all signals in the closed-loop system are bounded for a fixed time, and
(ii) the system output y follows the desired reference signal y_d.

To achieve control objectives, certain assumptions and lemmas are established.

Assumption 1. There exist positive constants $\bar{K}$ and $\bar{L}$ such that $\bar{K} < K(t) \leq 1$ and $|L(t)| \leq \bar{L}$.

Assumption 2. The reference signal y_d and its derivatives up to the ith order, denoted as $y_d^{(i)}$, are bounded and continuous for $i = 1, 2, \ldots, n$.

Assumption 3. The signs of $g_i(\cdot)$, where $1 \leq i \leq n$, are known, and there exist two constants $b_m > 0$ and $b_M > 0$ such that $b_m \leq |g_i(\cdot)| \leq b_M$. It is assumed, without loss of generality, that $0 < b_m \leq g_i(\cdot)$.

Assumption 4. The external disturbance $d_i(t)$ is required to satisfy $|d_i(t)| < d_i^*$, where the constants $d_i^* > 0$ are unknown for $i = 1, \ldots, n$.

Assumption 5. There exist nonnegative smooth functions $\psi_{i1}(\cdot)$ and $\psi_{i2}(\cdot)$ with $\psi_{i2}(0) = 0$ for $i = 1, \ldots, n$ such that

$$|\phi_i| \leq \psi_{i1}(|\bar{\chi}_i|) + \psi_{i2}(|z|). \tag{8}$$

Assumption 6. The dynamics described by $\dot{z} = q(z, \chi)$ are defined as exponentially input-state-practical stability (exp-ISpS), indicating the existence of an exp-ISpS Lyapunov function $V(z)$. This function must meet the following conditions:

$$\theta_1(|z|) \leq V(z) \leq \theta_2(|z|), \tag{9}$$

$$\frac{\partial V(z)}{\partial z} q(z, \chi) \leq -k_0 V(z) + \gamma(|\xi_1|) + d_0, \tag{10}$$

where $k_0 > 0$ and $d_0 > 0$ are known scalars, and θ_1, θ_2, and γ are K_∞-functions.

Remark 2. Assumption 1 is often used in control problems for nonlinear systems subject to actuator faults, as explained in [40]. On the other hand, the Assumption 2 is commonly used in tracking problems in control systems [36,37] to simplify stability analysis. For system (1) to satisfy the controllability requirement, it is necessary that the control gains $g_i(\bar{\chi}_i)$ are nonzero, and without loss of generality, can be assumed positive. This makes Assumption 3 reasonable. The lower bound b_m mainly serves purposes of stability and convergence analysis [49]. Assumption 4 introduces a practical consideration to system analysis and control design by implying bounded external disturbances [45]. Assumption 5 posits that the dynamic disturbances ϕ_i are bounded by the combined influence of $\psi_{i1}(|\bar{\chi}_i|)$ and $\psi_{i2}(|z|)$. It's important to note that both $\psi_{i1}(|\bar{\chi}_i|)$ and $\psi_{i2}(|z|)$ fall within the class K_∞, signifying that ϕ_i remains within bounds as long as χ_1 and z are bounded [36]. Assumption 6 asserts that the unmodeled dynamics of z exhibit ISpS. With this assumption, one can design a dynamic signal to effectively handle the unmodeled dynamics [36].

Definition 1 (Ref. [36])**.** Consider a nonlinear system as follows:

$$\dot{\chi} = f(\chi, t), \quad \chi(0) = \chi_0 \tag{11}$$

where $f(\cdot)$ is a nonlinear function and $\chi \in \mathbb{R}^n$ is a system variable. Suppose the system (11) is stable under a Lyapunov function, if there exists a convergence time T such that for all $t \geq T$, $\chi(t) = 0$, then system (11) demonstrates finite-time stability. Moreover, if the convergence time T is bounded by a fixed upper bound T_m, which is independent of the initial state, then system (11) is characterized by fixed-time stability.

Remark 3. The primary distinction between fixed-time stability and finite-time stability is their settling time characteristics. The settling time in finite-time stability [36–38] is bounded by the initial state and increases indefinitely. On the other hand, regardless of the initial conditions, fixed-time stability guarantees that the settling time is bounded and constant.

Lemma 1 ([36]). *For real numbers x, y, and positive constants c_1, c_2, c_3, one has*

$$|x|^{c_1}|y|^{c_2} \leq \frac{c_1}{c_1+c_2}c_3|x|^{c_1+c_2} + \frac{c_1}{c_1+c_2}c_3^{-\frac{c_1}{c_2}}|y|^{c_1+c_2}. \tag{12}$$

Lemma 2 ([36]). *Consider system (11). If there exist design constants $r_1 > 0$, $r_2 > 0$, $p > 1$, $0 < s < 1$, and $\beta \geq 0$, and a continuously differentiable function $V(\chi) > 0$ such that*

$$\dot{V}(\chi) \leq -r_1 V^p(\chi) - r_2 V^s(\chi) + \beta, \quad \forall \chi \in \mathcal{D} \subseteq \mathbb{R}^n, \tag{13}$$

then the system (11) is fixed-time stable on the set $\mathcal{D}$ with settling time

$$T \leq T_m := \frac{1}{r_1\Phi(p-1)} + \frac{1}{r_2\Phi(1-s)}. \tag{14}$$

The trajectories of (11) converge to the residual set

$$\chi \in \left\{ V(\chi) \leq \min\left[\left(\frac{\beta}{(1-\Phi)r_1}\right)^{\frac{1}{p}}, \left(\frac{\beta}{(1-\Phi)r_2}\right)^{\frac{1}{s}} \right] \right\}. \tag{15}$$

Here, $\mathcal{D}$ is a sufficiently large compact set containing the initial conditions.

Lemma 3 (Ref. [36]). *For any $c > 1$ and $x_i \geq 0$, the following inequality holds:*

$$\left(\sum_{i=1}^{N}|x_i|\right)^c \leq \sum_{i=1}^{N}|x_i|^c \leq N^{1-c}\left(\sum_{i=1}^{N}|x_i|\right)^c \tag{16}$$

Lemma 4 ([29]). *For $x, y \in \mathbb{R}$, one has*

$$xy \leq \frac{\varepsilon^p}{p}|x|^p + \frac{1}{q\varepsilon^q}|y|^q, \tag{17}$$

where $\varepsilon > 0$, $p > 1$, $q > 1$, and $(p-1)(q-1) = 1$.

Lemma 5 ([36]). *Suppose V serves as an exp-ISpS Lyapunov function for the subsystem $\dot{z} = q(z, \chi)$, where inequalities (9) and (10) are satisfied. For any constant $\bar{a} \in (0, a_o)$, and given an initial condition $z_0 = z(t_0)$, any function $\bar{\gamma}(|\chi_1|) \geq \gamma(|\chi_1|)$, there exists a nonnegative function $D(t)$, a finite time $T_0 = T_0(\bar{a}, r_0, z_0)$, and a dynamic signal described as*

$$\dot{r} = -\bar{a}r + \bar{\gamma}(|\chi_1|) + d, \quad r(0) = r_0 \tag{18}$$

such that $D(t) = 0$ for all $t \geq T_0$ and $V(z) \leq r(t) + D(t)$. The function $D(t)$ is given by

$$D(t) = \max\{0, e^{-a(t-t_0)}V(z_0) - e^{-\bar{a}(t-t_0)}v_0\}. \tag{19}$$

Without losing generality, assume that $\bar{\gamma}(s) = s^2\gamma_0(s^2)$, with $\gamma_0(s^2) > 0$ is a continuous function. Now, (18) can be rewritten as

$$\dot{r} = -\bar{a}r + \chi_1^2\gamma_0(|\chi_1^2|) + d, \quad r(0) = r_0. \tag{20}$$

Lemma 6 ([36]). *There exists a positive constant ζ such that for any $x \in \mathbb{R}$, the inequality*

$$|x| \leq x\tanh(x/\zeta) \leq \sigma\zeta \tag{21}$$

holds, where $\sigma = 0.2785$.

Lemma 7 ([36]). *For any constant $\nu > 0$, consider the set Ω_{z_1} defined as $\Omega_{z_1} := \{z_1 \mid |z_1| < 0.8814\nu\}$. Then, for every $z_1 \notin \Omega_{z_1}$, the inequality $1 - 2\tanh^2\left(\frac{z_1}{\nu}\right) \leq 0$ holds.*

2.1. Neural networks

In this work, the unknown functions are approximated by RBFNNs. As mentioned in [36], for a continuous nonlinear function $f(Z)$ defined in a compact set $\Omega_Z \subset \mathbb{R}^q$, there exists a neural network $W^{*T}S(Z)$ and constant $\varepsilon > 0$ such that

$$f(Z) = W^{*T}S(Z) + \delta(Z), \quad |\delta(Z)| \leq \varepsilon \tag{22}$$

With $\delta(Z)$ being the approximation error and W^* being the ideal constant weight vector and defined as

$$W^* := \arg\min_{W\in\mathbb{R}^l}\left\{\sup_{Z\in\Omega_Z}|f(Z) - W^TS(Z)|\right\}, \tag{23}$$

with $W = [w_1, w_2, \ldots, w_l]^T \in \mathbb{R}^l$ and $S(Z) = [s_1(Z), s_2(Z), \ldots, s_l(Z)]^T$ represents the basis function vector with

$$s_i(Z) = \exp\left(-\frac{(Z-\mu_i)^T(Z-\mu_i)}{\tau^2}\right), \tag{24}$$

where $\mu_i = [\mu_{i1}, \mu_{i2}, \ldots, \mu_{iq}]^T$ represents the center, and τ denotes the width of the Gaussian function.

Lemma 8 ([36]). *Define $S(Z) = [s_1(Z), \dots, s_l(Z)]^T$ as the basis function vector of an RBFNN, and let $Z = [z_1, \dots, z_n]^T$. For any positive integer $m \le n$, consider $Z_m = [z_1, \dots, z_m]^T$. Then*

$$||S(Z)||^2 \le ||S(Z_m)||^2. \tag{25}$$

3. Controller design and stability analysis

This section focuses on developing an adaptive fixed-time controller utilizing the backstepping technique. Before proceeding, the following coordinate transformation needs to be defined:

$$z_i = \chi_i - \varsigma_{i-1}, \quad i = 1, 2, \dots, n \tag{26}$$

where ς_{i-1} represents the virtual control law to be designed later, with $\varsigma_0 = y_d$.
Step 1: According to (1) and (26), we have

$$\begin{aligned} \dot{z}_1 &= \dot{\chi}_1 - \dot{y}_d \\ &= g_1\chi_2 + f_1 + \phi_1 + d_1 - \dot{y}_d. \end{aligned} \tag{27}$$

Chose the Lyapunov function candidate as follows:

$$V_1 = \frac{z_1^2}{2} + \frac{1}{\kappa_0} r + \frac{b_m}{2\kappa_1}\tilde{\eta}_1^2 \tag{28}$$

where $\kappa_0 > 0$ and $\kappa_1 > 0$ are design parameters, while b_m is specified in Assumption 3. The term $\tilde{\eta}_1 = \eta_1 - \hat{\eta}_1$ denotes the estimation error, where $\hat{\eta}_1$ is an adjustable parameter used for estimating the unknown constant η_1, which will be specified later.
By differentiating V_1 and using Assumption 5 and (20), one has

$$\begin{aligned} \dot{V}_1 = {} & z_1\left(g_1 z_2 + \varsigma_1 + f_1 + \phi_1 + d_1 - \dot{y}_d\right) + |\chi_1|\psi_{11}\left(|\chi_1|\right) + |z_1|\psi_{12}(|z|) \\ & + \frac{1}{\kappa_0}\left(\chi_1^2\psi_0\left(\chi_1^2\right) + d\right) - \frac{\bar{a}}{\kappa_0} r - \frac{1}{\kappa_1}\tilde{\eta}_1\dot{\hat{\eta}}_1. \end{aligned} \tag{29}$$

Applying Lemma 4 and Assumption 4, one has

$$z_1 d_1 \le \frac{1}{2} z_1^2 + \frac{d_1^{*2}}{2}. \tag{30}$$

Next, the terms $|\chi_1|\psi_{11}\left(|\chi_1|\right)$ and $|z_1|\psi_{12}(|z|)$ in (29) are handled. By using Lemma 6, it follows that

$$\begin{aligned} |\chi_1|\psi_{11}\left(|\chi_1|\right) &\le \sigma_1^{'} + z_1\psi_{11}\left(|\chi_1|\right)\tanh\left(\frac{z_1\psi_{11}\left(|\chi_1|\right)}{\sigma_1}\right) \\ &= e_1\hat{\psi}_{11}(x_1) + \sigma_1^{'}, \end{aligned} \tag{31}$$

where $\sigma_1^{'} = 0.2785\sigma_1$ and $\hat{\psi}_{11}(\chi_1) = \psi_{11}\left(|\chi_1|\right)\tanh\left(\frac{z_1\psi_{11}\left(|\chi_1|\right)}{\sigma_1}\right)$ is a smooth function. Similar to the methods used in [36], one has

$$\begin{aligned} |z_1|\psi_{12}(|z|) &\le |z_1|\bar{\psi}_{12}(r) + \frac{1}{4} z_1^2 + b_1(t) \\ &\le z_1\bar{\psi}_{12}(r)\tanh\left(\frac{z_1\bar{\psi}_{12}(r)}{\iota_1}\right) + \iota_1^{'} + \frac{1}{4} z_1^2 + b_1(t) \\ &= z_1\hat{\psi}_{12}(\chi_1, r) + \iota_1^{'} + \frac{1}{4} z_1^2 + b_1(t), \end{aligned} \tag{32}$$

where $\iota_1^{'} = 0.2785\iota_1$ and $\hat{\psi}_{12}(r) = \psi_{12}\circ\theta_1^{-1}(2r)$, $b_1(t) = (\kappa_{12}\circ\theta_1^{-1}(2D(t)))^2$, and $\hat{\psi}_{12}(\chi_1, r) = \bar{\chi}_{12}(r)\tanh\left(\frac{z_1\bar{\psi}_{12}(r)}{\iota_1}\right)$ with $b_1(t) \ge 0$ for all $t \ge 0$.
By using (30)–(32)into (29), one has

$$\begin{aligned} \dot{V}_1 \le {} & z_1(g_1 z_2 + \bar{f}_1(Z_1) - \frac{1}{2} z_1^2 + (1 - 2\tanh^2(z_1/\nu))\frac{\chi_1^2\gamma_0(\chi_1^2)}{\kappa_0} - \frac{1}{\kappa_1}\tilde{\eta}_1\dot{\hat{\eta}}_1 - \frac{\bar{a}}{\kappa_0} r + \sigma_1^{'} \\ & + \frac{d}{\kappa_0} + \iota_1^{'} + b_1(t) + \frac{d_i^{*2}}{2}, \end{aligned} \tag{33}$$

where

$$\bar{f}_1(Z_1 + = \frac{1}{2} z_1 + f_1 - \dot{y}_d + \hat{\psi}_{11}(\chi_1) + \hat{\psi}_{12}(\chi_1, r) + \frac{2}{z_1}\tanh^2(z_1/\nu))\frac{\chi_1^2\psi_0(x_1^2)}{\kappa_0} + \frac{1}{4} z_1. \tag{34}$$

Since $\bar{f}_1(Z_1)$ includes the unknown functions f_1 and g_1, an RBFNN is utilized to approximate them. According to (22), for any $\varepsilon_1 > 0$, there exists a neural network $W_1^{*T} P_1(Z_1)$ such that

$$\bar{f}_1(Z_1) = W_1^{*T} P_1(Z_1) + \delta_1(Z_1), \quad |\delta_1(Z_1)| \le \varepsilon_1 \tag{35}$$

with $Z_1 = [\chi_1, \ldots, \chi_n, y_d, \dot{y}_d, r]^T$.

Applying Lemmas 4 and 8, one obtain

$$\begin{aligned} z_1 \bar{f}_1(Z_1) &= z_1(W_1^{*T} P_1(X_1) + \delta_1(Z_1)) \\ &\leq \frac{1}{2b_1^2} z_1^2 \|W_1^*\|^2 P_1^T(Z_1) P_1(Z_1) + \frac{a_1^2}{2} + \frac{z_1^2}{2} + \frac{\varepsilon_1^2}{2} \\ &\leq \frac{b_m}{2a_1^2} z_1^2 \eta_1 P_1^T(X_1) P_1(X_1) + \frac{a_1^2}{2} + \frac{z_1^2}{2} + \frac{\varepsilon_1^2}{2} \end{aligned} \tag{36}$$

with $a_1 > 0$ being a design parameter and $\eta_1 = \frac{\|W_1^*\|^2}{b_m}$, and $X_1 = [\chi_1, y_d, \dot{y}_d, r]^T$.

Construct the virtual controller as follows:

$$\varsigma_1 = -k_1 z_1^{2\alpha-1} - q_1 z_1^{2\beta-1} - \frac{1}{2a_1^2} \hat{\eta}_1 z_1 P_1^T(X_1) P_1(X_1). \tag{37}$$

with $\alpha > 1$, $\beta \in (0, 1)$, $k_1 > 0$, $q_1 > 0$, and $a_1 > 0$ being the design parameters.
Construct the adaptive law as follows:

$$\dot{\hat{\eta}}_1 = \frac{\kappa_1}{2a_1^2} z_1^2 P_1^T(X_1) P_1(X_1) - \varrho_1 \hat{\eta}_1 - \bar{\varrho}_1 \hat{\eta}_1 \tag{38}$$

with $\kappa_1 > 0$, $a_1 > 0$, $\varrho_1 > 0$, and $\bar{\varrho}_1 > 0$ being the design parameters.
By using (36)–(38) into (33), yields

$$\begin{aligned} \dot{V}_1 \leq & -k_1 b_m z_1^{2\alpha} - q_1 b_m z_1^{2\beta} - \frac{\bar{a}}{\kappa_0} r + \frac{a_1^2}{2} + \frac{\varepsilon_1^2}{2} + (1 - 2\tanh^2(z_1/\nu)) \frac{\chi_1^2 \gamma_0(\chi_1^2)}{\kappa_0} \\ & + \frac{\varrho_1}{\kappa_1} \tilde{\eta}_1 \hat{\eta}_1 + \frac{\bar{\varrho}_1}{\kappa_1} \tilde{\eta}_1 \hat{\eta}_1 + \frac{d}{\kappa_0} + \iota_1' + \sigma_1' + b_1(t) + \frac{d_i^{*2}}{2} + g_1 z_1 z_2 \end{aligned} \tag{39}$$

Step i $(2 \leq i \leq n-1)$: Based on (1) and (26), one has

$$\begin{aligned} \dot{z}_i &= \dot{\chi}_i - \dot{\varsigma}_{i-1} \\ &= g_i \chi_{i+1} + f_i + \phi_i + d_i - \dot{\varsigma}_{i-1} \end{aligned} \tag{40}$$

where

$$\dot{\varsigma}_{i-1} = \sum_{j=1}^{i-1} \frac{\partial \varsigma_{i-1}}{\partial \chi_j} \phi_j + \Xi_{i-1} \tag{41}$$

with

$$\Xi_{i-1} = \sum_{j=1}^{i-1} \frac{\partial \varsigma_{i-1}}{\partial \chi_j} (f_j + g_j \chi_{j+1}) + \sum_{j=1}^{i-1} \frac{\partial \varsigma_{i-1}}{\partial \hat{\eta}_j} \dot{\hat{\eta}}_j + \sum_{j=0}^{i-1} \frac{\partial \varsigma_{i-1}}{\partial y_d^{(i)}} y_d^{(j+1)} + \frac{\partial \varsigma_{i-1}}{\partial r} \dot{r}. \tag{42}$$

Take the Lyapunov function candidate as follows:

$$V_i = V_{i-1} + \frac{1}{2} z_i^2 + \frac{b_m}{2\kappa_i} \tilde{\eta}_i^2, \tag{43}$$

where $\kappa_i > 0$ denotes a design parameter, while b_m is specified in Assumption 3. The term $\tilde{\eta}_i = \eta_i - \hat{\eta}_i$ denotes the estimation error, where $\hat{\eta}_i$ is an adjustable parameter used for estimating the unknown constant η_i, which will be specified later.
By differentiating V_i, yields

$$\dot{V}_i = \dot{V}_{i-1} + z_i(g_i z_{i+1} + g_i \varsigma_i + f_i + \bar{\phi}_i + d_i - \Xi_{i-1}) - \frac{1}{\lambda_i} \tilde{\eta}_i \dot{\hat{\eta}}_i. \tag{44}$$

where $\bar{\phi}_i = \phi_i - \sum_{j=1}^{i-1} \frac{\partial \varsigma_{i-1}}{\partial \chi_j} \phi_j$ and $\dot{V}_{i-1}$ fulfills the following result, which can be attained by utilizing a methodology similar to step 1.

$$\begin{aligned} \dot{V}_{i-1} \leq & -\sum_{j=1}^{i-1} k_j b_m z_j^{2\alpha} - \sum_{j=1}^{i-1} q_j b_m z_j^{2\beta} - \frac{\bar{a}}{\kappa_0} r + \sum_{j=1}^{i-1} \left(\frac{a_j^2}{2} + \frac{\varepsilon_j^2}{2} + \iota_j' + \sigma_j' + b_j(t) + \frac{d_j^{*2}}{2} \right) \\ & + (1 - 2\tanh^2(z_1/\nu)) \frac{\chi_1^2 \gamma_0(\chi_1^2)}{\kappa_0} + \sum_{j=1}^{i-1} \frac{\varrho_j}{\kappa_j} \tilde{\eta}_j \hat{\eta}_j + \sum_{j=1}^{i-1} \frac{\bar{\varrho}_j}{\kappa_j} \tilde{\eta}_j \hat{\eta}_j + \frac{d}{\kappa_0}. \end{aligned} \tag{45}$$

Applying Lemma 4 and Assumption 4, one has

$$z_i d_i \leq \frac{1}{2} z_i^2 + \frac{d_i^{*2}}{2}. \tag{46}$$

By using Assumption 5, one has

$$\begin{aligned}|z_i\bar{\phi}_i| &\le |z_i|\left(|\phi_i| + \sum_{j=1}^{i-1}\left|\frac{\partial \varsigma_{i-1}}{\partial \chi_j}\right||\phi_i|\right)\\ &\le |z_i|\left(\psi_{i1}(|\bar{\chi}_i|) + \sum_{j=1}^{i-1}\left|\frac{\partial \varsigma_{i-1}}{\partial \chi_j}\right|\psi_{j1}(|\chi|)\right)\\ &\quad + |z_i|\left(\psi_{i2}(|z|) + \sum_{j=1}^{i-1}\left|\frac{\partial \varsigma_{i-1}}{\partial \chi_j}\right|\psi_{j2}(|z|)\right).\end{aligned} \tag{47}$$

Similar to (31), we have

$$|z_i|\left(\psi_{i1}(|\bar{\chi}_i|) + \sum_{j=1}^{i-1}\left|\frac{\partial \varsigma_{i-1}}{\partial \chi_j}\right|\psi_{j1}(|\bar{\chi}_i|)\right) \le z_i\hat{\psi}_{i1}(\bar{\chi}_i, \hat{\eta}_{i-1}, r) + \sigma_i^{'}, \tag{48}$$

where $\sigma_i^{'} = 0.2785\sigma_i$ and $\hat{\psi}_{i1}(\chi, \hat{\eta}_{i-1}, r) = \left(\psi_{i1} + \sum_{j=1}^{i-1}\left|\frac{\partial \varsigma_{i-1}}{\partial \chi_j}\right|\psi_{j1}\right)\tanh\left(z_i\left(\psi_{i1} + \sum_{j=1}^{i-1}\left|\frac{\partial \varsigma_{i-1}}{\partial \chi_j}\right|\psi_{j1}/\sigma_i\right)\right)$.

Similar to the (32), one has

$$|z_i|\left(\psi_{i2}(|z|) + \sum_{j=1}^{i-1}\left|\frac{\partial \varsigma_{i-1}}{\partial \chi_j}\right|\psi_{j2}(|z|)\right) \le \frac{z_i^2}{4}\left(1 + \sum_{j=1}^{i-1}\left(\frac{\partial \varsigma_{i-1}}{\partial \chi_j}\right)^2\right) + z_i\hat{\psi}_{i2}(\chi, \hat{\eta}_{i-1}, r) + \iota_i^{'} + b_i(t), \tag{49}$$

where $\iota_i^{'} = 0.2785\iota_i$ and $\hat{\psi}_{i2}(\chi, \hat{\eta}_{i-1}, r) = \bar{\psi}_{i2}(\bar{\chi}_i, \hat{\eta}_{i-1}, r)\tanh\left(\frac{z_i\bar{\psi}_{i2}(\chi, \hat{\eta}_{i-1}, r)}{\iota_i}\right)$, $\bar{\psi}_{i2}(\bar{\chi}_i, \hat{\eta}_{i-1}, r) = \psi_{i2}\circ\theta_1^{-1}(2r) + \sum_{j=1}^{i-1}\left|\frac{\partial \varsigma_{i-1}}{\partial \chi_j}\right|\psi_{i2}\circ\theta_1^{-1}(2r)$, and $b_i(t) = \sum_{j=1}^{i}(\psi_{j2}\circ\theta_1^{-1}(2D))^2$ with $b_i(t) \ge 0$ for all $t \ge 0$.
Substituting (45)–(49) into (44), one has

$$\begin{aligned}\dot{V}_i \le &-\sum_{j=1}^{i-1}k_j b_m z_j^{2\alpha} - \sum_{j=1}^{i-1}q_j b_m z_j^{2\beta}\\ &-\frac{\bar{a}}{\kappa_0}r + z_i\left(g_i\varsigma_i + \bar{f}_i(Z_i)\right)\sum_{j=1}^{i-1}\left(\frac{a_j^2}{2} + \frac{\epsilon_j^2}{2} + \iota_j^{'} + \sigma_j^{'} + b_j(t) + \frac{d_j^{*2}}{2}\right)\\ &+ (1 - 2\tanh^2(z_1/\nu))\frac{\chi_1^2\gamma_0(\chi_1^2)}{\kappa_0} + \sum_{j=1}^{i-1}\frac{\varrho_j}{\kappa_j}\tilde{\eta}_j\hat{\eta}_j + \sum_{j=1}^{i-1}\frac{\bar{\varrho}_j}{\kappa_j}\tilde{\eta}_j\hat{\eta}_j + \frac{d}{\kappa_0} + \iota_i^{'} + \sigma_i^{'} + b_i(t) + \frac{d_i^{*2}}{2}\end{aligned} \tag{50}$$

where

$$\bar{f}_i(X_i) = g_i z_{i+1} + f_i - \Xi_{i-1} + \hat{\psi}_{i1}(\bar{\chi}_i, \hat{\eta}_{i-1}, r) + \hat{\psi}_{12}(\bar{\chi}_i, \hat{\eta}_{i-1}, r). \tag{51}$$

Since $\bar{f}_i(Z_i)$ contains the unknown functions f_i and g_i, an RBFNN is utilized to approximate them. Based on (22), for any $\epsilon_i > 0$, there exists a neural network $W_i^{*T}P_i(Z_i)$ such that

$$\bar{f}_i(Z_i) = W_i^{*T}P_i(Z_i) + \delta_i(Z_1), \quad |\delta_i(Z_i)| \le \epsilon_i \tag{52}$$

where $Z_i = [\chi_1, \dots \chi_n, \tilde{\eta}_{i-1}^T, \bar{y}_d^{(i)}, r]^T$ with $\tilde{\eta}_{i-1}^T = [\hat{\eta}_1, \dots, \hat{\eta}_{i-1}]^T$ and $\bar{y}_d^{(i)}]^T = [y_d, \dots, y_d^{(i)}]^T$, respectively.
By using Lemmas 4 and 8, one has

$$\begin{aligned}z_i\bar{f}_i(Z_i) &= z_i(W_i^{*T}P_i(Z_i) + \delta_i(Z_i))\\ &\le \frac{1}{2a_i^2}z_i^2\|W_i^*\|^2P_i^T(Z_i)P_i(Z_i) + \frac{a_i^2}{2} + \frac{z_i^2}{2} + \frac{\epsilon_i^2}{2}\\ &\le \frac{b_m}{2a_i^2}z_i^2\eta_i P_i^T(X_i)P_i(X_i) + \frac{a_i^2}{2} + \frac{z_i^2}{2} + \frac{\epsilon_i^2}{2}\end{aligned} \tag{53}$$

where b_m is specified in Assumption 3, while $a_i > 0$ denotes a tunable design parameter. The term η_i is defined as $\eta_i = \frac{\|W_i^*\|^2}{b_m}$, and the vector X_i is given by $X_i = [\bar{\chi}_i^T, \tilde{\eta}_{i-1}^T, \bar{y}_d^{(i)}, r]^T$, where $\bar{\chi}_i = [\chi_1, \dots, \chi_i]^T$.
Construct the virtual controller ς_i as follows:

$$\varsigma_i = -k_i z_i^{2\alpha-1} - q_i z_i^{2\beta-1} - \frac{1}{2a_i^2}\hat{\eta}_i z_i P_i^T(X_i)P_i(X_i), \tag{54}$$

with $\alpha > 1$, $\beta \in (0, 1)$, $k_i > 0$, $q_i > 0$, and $a_i > 0$ being the design parameters.
Construct the adaptive law as follows:

$$\dot{\hat{\eta}}_i = \frac{\kappa_i}{2a_i^2}z_i^2P_i^T(X_i)P_i(X_i) - \varrho_i\hat{\eta}_i - \bar{\varrho}_i\hat{\eta}_i \tag{55}$$

where $\kappa_i > 0$, $\varrho_i > 0$ and $\bar{\varrho}_i > 0$ are the design parameters.
By inserting (53)–(55) into (50), one has

$$\begin{aligned}\dot{V}_i \leq & -\sum_{j=1}^{i} k_j b_m z_j^{2\alpha} - \sum_{j=1}^{i} q_j b_m z_j^{2\beta} - \frac{\bar{a}}{\kappa_0} r + (1 - 2\tanh^2(z_1/\nu)) \frac{\chi_1^2 \gamma_0(\chi_1^2)}{\kappa_0} \\ & + \sum_{j=1}^{i} \frac{\varrho_j}{\kappa_j} \tilde{\eta}_j \hat{\eta}_j + \sum_{j=1}^{i} \frac{\bar{\varrho}_j}{\kappa_j} \tilde{\eta}_j \hat{\eta}_j + \frac{d}{\kappa_0} + \sum_{j=1}^{i} \left(\frac{a_j^2}{2} + \frac{\varepsilon_j^2}{2} + \iota_j' + \sigma_j' + b_j(t) + \frac{d_j^{*2}}{2} \right)\end{aligned} \tag{56}$$

Step n: According to (1), (2), (4), and (26), one has

$$\begin{aligned}\dot{z}_n &= \dot{\chi}_n - \dot{\varsigma}_{n-1} \\ &= g_n u^f + f_n + \phi_n + d_n(t) - \dot{\varsigma}_{n-1} \\ &= g_n(K(t)m(t)\upsilon + K(t)\beta(t) + L(t)) + f_n + \phi_n + d_n(t) - \dot{\varsigma}_{n-1} \\ & g_n K(t)m(t)\upsilon + g_n K(t)\beta(t) + g_n L(t) + f_n + \phi_n + d_n(t) - \dot{\varsigma}_{n-1}\end{aligned} \tag{57}$$

where $\dot{\varsigma}_{n-1}$ is defined in (41) with $i = n$.
Chose the candidate of Lyapunov function as follows:

$$V_n = V_{n-1} + \frac{1}{2} z_n^2 + \frac{b_m}{2\kappa_n} \tilde{\eta}_n^2, \tag{58}$$

where $\kappa_n > 0$ denotes a design parameter, while b_m is specified in Assumption 3. The term $\tilde{\eta}_n = \eta_n - \hat{\eta}_n$ denotes the estimation error, where $\hat{\eta}_n$ is an adjustable parameter used for estimating the unknown constant η_n, which will be specified later.
The dynamic equation of V_n is

$$\dot{V}_n = \dot{V}_{n-1} + g_n K(t)m(t)\upsilon + g_n K(t)\beta(t) + g_n L(t) + f_n + d_n(t) + \bar{\phi}_n - \Xi_{n-1} - \frac{1}{\kappa_n} \tilde{\eta}_n \dot{\hat{\eta}}_n, \tag{59}$$

where $\bar{\phi}_n = \phi_n - \sum_{j=1}^{n-1} \frac{\partial \varsigma_{n-1}}{\partial \chi_j} \phi_j$ and $\dot{V}_{n-1}$ defined in (45) with $i = n$.
Utilizing the same estimation techniques as described in Eqs. (47) through (49), one has

$$\begin{aligned}\left| z_n \bar{\phi}_n \right| \leq & \, z_n \hat{\psi}_{n1}(\bar{\chi}_n, \hat{\eta}_{n-1}, r) + z_n \hat{\psi}_{n2}(\bar{\chi}_n, \hat{\eta}_{n-1}, r) \\ & + \frac{z_i^2}{4} \left(1 + \sum_{j=1}^{n-1} \left(\frac{\partial \varsigma_{i-1}}{\partial \chi_j} \right)^2 \right) + \sigma_n' + \iota_n' + b_n(t),\end{aligned} \tag{60}$$

where $\hat{\psi}_{n1}(\bar{\chi}_n, \hat{\eta}_{n-1}, r)$ and $\hat{\psi}_{n2}(\bar{\chi}_n, \hat{\eta}_{n-1}, r)$ are defined in (48) and (49), respectively, and $b_n(t) \geq 0$ for all $t \geq 0$.
Applying Lemma 4 and Assumption 4, one has

$$z_n d_n \leq \frac{1}{2} z_n^2 + \frac{d_n^{*2}}{2}. \tag{61}$$

Applying Lemma 4 and Assumptions 1 and 3 with (7), one has

$$z_n g_n K(t)\beta(t) \leq \frac{1}{2} z_n^2 + \frac{b_m \bar{\beta}^2}{2}. \tag{62}$$

Similarly, applying Lemma 4 and Assumptions 1, one has

$$z_n g_n L(t) \leq \frac{1}{2} z_n^2 + \frac{b_m \bar{L}^2}{2}. \tag{63}$$

By using (60)–(63) into (59), one has

$$\begin{aligned}\dot{V}_n \leq & -\sum_{j=1}^{n-1} k_j b_m z_j^{2\alpha} - \sum_{j=1}^{n-1} q_j b_m z_j^{2\beta} - \frac{\bar{a}}{\kappa_0} r \\ & + z_n \left(g_n K(t)m(t)\upsilon + \bar{f}_n(Z_n) \right) \sum_{j=1}^{n-1} \left(\frac{a_j^2}{2} + \frac{\varepsilon_j^2}{2} + \iota_j' + \sigma_j' + b_j(t) + \frac{d_j^{*2}}{2} \right) \\ & + (1 - 2\tanh^2(z_1/\nu)) \frac{\chi_1^2 \gamma_0(\chi_1^2)}{\kappa_0} + \sum_{j=1}^{n-1} \frac{\varrho_j}{\kappa_j} \tilde{\eta}_j \hat{\eta}_j \\ & + \sum_{j=1}^{n-1} \frac{\bar{\varrho}_j}{\kappa_j} \tilde{\eta}_j \hat{\eta}_j + \frac{d}{\kappa_0} + \iota_n' + \sigma_n' + b_n(t) + \frac{d_n^{*2}}{2} + \frac{b_m \bar{\beta}^2}{2} + \frac{b_m \bar{L}^2}{2} - \frac{1}{2} z_n^2,\end{aligned} \tag{64}$$

where

$$\bar{f}_n(Z_n) = f_n - \dot{\Xi}_{n-1} + 2z_n. \tag{65}$$

Since $\bar{f}_n(Z_n)$ includes the unknown functions f_n and g_n, an RBFNN is utilized to approximate it. According to (22), for any $\epsilon_n > 0$, there exists a neural network $W_n^{*T} P_n(Z_n)$ such that

$$\bar{f}_n(Z_n) = W_n^{*T} P_n(Z_n) + \delta_n(Z_n), \quad |\delta_n(Z_n)| \leq \epsilon_n \tag{66}$$

where $Z_n = [\zeta_1, \ldots, \zeta_n, \bar{\hat{\eta}}_{n-1}^T, \bar{y}_d^{(n)}, r]^T$ with $\bar{\hat{\eta}}_{n-1}^T = [\hat{\eta}_1, \ldots, \hat{\eta}_{n-1}]^T$ and $\bar{y}_d^{(n)}]^T = [y_d, \ldots, y_d^{(n)}]^T$, respectively.
By using Lemmas 4 and 8, one has

$$\begin{aligned} z_n \bar{f}_n(Z_n) &= z_n(W_n^{*T} P_n(Z_n) + \delta_n(Z_n)) \\ &\leq \frac{1}{2a_n^2} z_n^2 \|W_n^*\|^2 P_n^T(Z_n) P_n(Z_n) + \frac{a_n^2}{2} + \frac{z_n^2}{2} + \frac{\epsilon_n^2}{2} \\ &\leq \frac{b_m}{2a_n^2} z_n^2 \eta_n P_n^T(X_n) P_n(X_n) + \frac{a_n^2}{2} + \frac{z_n^2}{2} + \frac{\epsilon_n^2}{2} \end{aligned} \tag{67}$$

where $\eta_n = \frac{\|W_i^*\|^2}{b_m}$, and $X_n = [\bar{\chi}_n^T, \bar{\hat{\eta}}_{n-1}^T, \bar{y}_d^{(n)}, r]^T$ with $\bar{\chi}_n = [\chi_1, \ldots, \chi_n]^T$, and $a_n > 0$ denotes a design parameter.
The actual control input υ is designed as follows:

$$\upsilon = -k_n z_n^{2\alpha_1} - q_n z_n^{2\beta-1} - \frac{1}{2a_n^2} \hat{\eta}_n z_n P_n^T(X_n) P_n(X_n), \tag{68}$$

with $\alpha > 1$, $\beta \in (0, 1)$, $k_n > 0$, $q_n > 0$, and $a_n > 0$ being the design parameters.
Construct the adaptive law as follows:

$$\dot{\hat{\eta}}_n = \frac{\kappa_n}{2a_n^2} z_n^2 P_n^T(X_n) P_n(X_n) - \varrho_n \hat{\eta}_n - \bar{\varrho}_n \hat{\eta}_n \tag{69}$$

where $\kappa > 0$, $\varrho > 0$, and $\bar{\varrho}_n > 0$ represent the design parameters.
By using Lemma 4, Assumptions 1 and 3 along with (7), one obtains

$$g_n K(t) m(t) \upsilon \leq -b_m \bar{m} k_n z_n^{2\alpha} - b_m \bar{m} q_n z_n^{2\beta} + \frac{1}{2a_n^2} e_n^2 \hat{\eta}_n P_n^T(X_n) P_n(X_n) \tag{70}$$

Substituting (67)–(70) into (64), one has

$$\begin{aligned} \dot{V}_n \leq & -\sum_{j=1}^{n} \left(c_j z_j^{2\alpha} \right) - \sum_{j=1}^{n-1} \left(\bar{c}_j z_j^{2\beta} \right) - \frac{\bar{a}}{\kappa_0} r + (1 - 2\tanh^2(z_1/\nu)) \frac{\chi_1^2 \gamma_0(\chi_1^2)}{\kappa_0} \\ & + \sum_{j=1}^{n} \frac{\varrho_j}{\kappa_j} \tilde{\eta}_j \hat{\eta}_j + \sum_{j=1}^{n} \frac{\bar{\varrho}_j}{\kappa_j} \tilde{\eta}_j \hat{\eta}_j + \frac{d}{\kappa_0} + \sum_{j=1}^{n} \left(\frac{a_j^2}{2} + \frac{\varepsilon_j^2}{2} + \iota_j' + \sigma_j' + b_j(t) + \frac{d_j^{*2}}{2} \right) \\ & + \frac{b_m \bar{\beta}^2}{2} + \frac{b_m \bar{L}^2}{2} \end{aligned} \tag{71}$$

where $c_j = k_j b_m + \bar{m} k_n b_m$ and $\bar{c}_j = q_j b_m + b_m \bar{m} q_n$ for $j = 1, \ldots, n-1$.

Theorem 1. *Consider the nonlinear system described in (1), subject to Assumptions 1–6. By implementing the virtual controllers (37) and (54), the actual control law (68), and the adaptive update rules (38), (55), and (69), the aim is to ensure boundedness of all signals in the closed-loop system and achieve convergence of the output to a small neighborhood around the origin within a fixed-time.*

Proof. It is noteworthy that

$$\frac{\varrho_j}{\kappa_j} \tilde{\eta}_j \hat{\eta}_j \leq -\frac{\varrho_j}{2\kappa_j} \tilde{\eta}_j^2 + \frac{\varrho_j}{2\kappa_j} \eta_j^2, \tag{72}$$

$$\frac{\bar{\varrho}_j}{\kappa_j} \tilde{\eta}_j \hat{\eta}_j \leq -\frac{\bar{\varrho}_j}{2\kappa_j} \tilde{\eta}_j^2 + \frac{\bar{\varrho}_j}{2\kappa_j} \eta_j^2. \tag{73}$$

By using (72)-(73) into (71), we have

$$\begin{aligned} \dot{V}_n \leq & -\sum_{j=1}^{n} \left(c_j e_j^{2\alpha} + \frac{\varrho_j}{2\kappa_j} \tilde{\eta}_j^2 \right) - \sum_{j=1}^{n} \left(\bar{c}_j e_j^{2\beta} + \frac{\bar{\varrho}_j}{2\kappa_j} \tilde{\eta}_j^2 \right) \\ & + (1 - 2\tanh^2(z_1/\nu)) \frac{\chi_1^2 \gamma_0(\chi_1^2)}{\kappa_0} - \frac{\bar{a}}{\kappa_0} r + \Delta \end{aligned} \tag{74}$$

where $\Delta = \sum_{j=1}^{n} \vartheta_j + \frac{b_m \bar{\beta}^2}{2} + \frac{b_m \bar{L}^2}{2} + \frac{d}{\kappa_0}$ with $\vartheta_j = \frac{\varrho_j}{2\kappa_j} \eta_j^2 + \frac{\bar{\varrho}_j}{2\kappa_j} \eta_j^2 \frac{a_j^2}{2} + \frac{\varepsilon_j^2}{2} + \iota_j' + \sigma_j' + b_j(t) + \frac{d_j^{*2}}{2}$, $j = 1, \ldots, n$.
By using Lemma 1, we have

$$\left(\sum_{j=1}^{n} \frac{\tilde{\eta}_j^2}{2\kappa_j} \right)^{\alpha} \leq \sum_{j=1}^{n} \frac{\tilde{\eta}_j^2}{2\kappa_j} + (1 - \alpha) \alpha^{\frac{\alpha}{1-\alpha}} \tag{75}$$

$$\left(\sum_{j=1}^{n}\frac{\tilde{\eta}_j^2}{2\kappa_j}\right)^{\beta}\leq\sum_{j=1}^{n}\frac{\tilde{\eta}_j^2}{2\kappa_j}+(1-\beta)\beta^{\frac{\beta}{1-\beta}} \tag{76}$$

By using (75) and (76) into (74), one has

$$\begin{aligned}\dot{V}_n&\leq-\sum_{j=1}^{n}c_j z_j^{2\alpha}-\sum_{j=1}^{n}\varrho_j\left(\frac{\tilde{\eta}_j^2}{2\kappa_j}\right)^{\alpha}-\sum_{j=1}^{n}\bar{c}_j z_j^{2\beta}-\sum_{j=1}^{n}\bar{\varrho}_j\left(\frac{\tilde{\eta}_j^2}{2\kappa_j}\right)^{\beta}\\&+(1-2\tanh^2(z_1/\nu))\frac{\chi_1^2\gamma_0(\chi_1^2)}{\kappa_0}+b_0\\&\leq-c\sum_{j=1}^{n}(\frac{1}{2}z_j^2)^{\alpha}-c\sum_{j=1}^{n}\left(\frac{\tilde{\eta}_j^2}{2\kappa_j}\right)^{\alpha}-\hat{c}\sum_{j=1}^{n}(\frac{1}{2}z_j^2)^{\beta}-k\sum_{j=1}^{n}\left(\frac{\tilde{\eta}_j^2}{2\kappa_j}\right)^{\beta}\\&+b_0+(1-2\tanh^2(z_1/\nu))\frac{\chi_1^2\gamma_0(\chi_1^2)}{\kappa_0}\end{aligned} \tag{77}$$

$c=\min\left\{2^{\alpha}c_j,\varrho_j,\bar{a}:1\leq j\leq n\right\},\quad \hat{c}=\min\left\{2^{\beta}\bar{c}_j,\bar{\varrho}_j,\bar{a}:1\leq j\leq n\right\},\quad b_0=\sum_{j=1}^{n}\vartheta_j+\frac{b_m\bar{\beta}^2}{2}+\frac{b_m\bar{L}^2}{2}++\frac{d}{\kappa_0}+(1-\alpha)\alpha^{\frac{\alpha}{1-\alpha}}+(1-\beta)\beta^{\frac{\beta}{1-\beta}}$

where $\vartheta_j=\frac{\varrho_j}{2\kappa_j}\eta_j^2+\frac{\bar{\varrho}_j}{2\kappa_j}\eta_j^2+\frac{a_j^2}{2}+\frac{\epsilon_j^2}{2}+\iota_j'+\sigma_j'+b_j(t)+\frac{d_j^{*2}}{2}$, for $j=1,\ldots,n$.

By using Lemma 3, we have

$$\begin{aligned}\dot{V}_n&\leq c\left(\sum_{j=1}^{n}\left(\frac{z_j^2}{2}+\frac{\tilde{\eta}_j^2}{2\kappa_j}\right)\right)^{\alpha}-\hat{c}\left(\sum_{j=1}^{n}\left(\frac{z_j^2}{2}+\frac{\tilde{\eta}_j^2}{2\kappa_j}\right)\right)^{\beta}\\&+b_0+(1-2\tanh^2(z_1/\nu))\frac{\chi_1^2\gamma_0(\chi_1^2)}{\kappa_0}\\&\leq-cV^{\alpha}(\chi)-kV^{\beta}(\chi)+b_0+(1-2\tanh^2(z_1/\nu))\frac{\chi_1^2\gamma_0(\chi_1^2)}{\kappa_0}.\end{aligned} \tag{78}$$

The significance of the last term $(1-2\tanh^2(z_1/\nu))\frac{\chi_1^2\gamma_0(\chi_1^2)}{\kappa_0}$ in (78) becomes apparent when analyzing the stability of the closed-loop system. We proceed to demonstrate the system's stability through two cases:

Case 1 When $z_1\in\{z_1\mid|z_1|<0.8814\nu\}$ with ν as a positive constant, the boundedness of χ_1 is evident from (26) with $i=1$ since z_1 and y_d are bounded variables. Additionally, $\gamma_0(\chi_1^2)$, being a non-negative smooth function, is also bounded. Consequently, the last term $(1-2\tanh^2(z_1/\nu))\frac{\chi_1^2\gamma_0(\chi_1^2)}{\kappa_0}$ is bounded and c_0 is assumed to be its bound. From (78), one has

$$V_n\leq-cV^{\alpha}(\chi)-kV^{\beta}(\chi)+\varkappa_0, \tag{79}$$

where $\varkappa_0=b_0+c_0$.

Case 2 When $z_1\notin\{z_1\mid|z_1|<0.8814\nu\}$, applying Lemma 7 and considering the non-negativity of $\chi_1^2\gamma_0(\chi_1^2)/\kappa_0$ leads to $(1-2\tanh^2(z_1/\nu))\frac{\chi_1^2\gamma_0(\chi_1^2)}{\kappa_0}\leq 0$.

Hence, (78) simplifies to

$$V_n\leq-cV^{\alpha}(\chi)-kV^{\beta}(\chi)+b_0. \tag{80}$$

Summarizing the two cases yields the following conclusion

$$V_n\leq-cV^{\alpha}(\chi)-kV^{\beta}(\chi)+\varkappa_0. \tag{81}$$

Utilizing Lemma 2, we can conclude that all system signals of (1) exhibit semi-global fixed-time stability and converge to the following compact residual set:

$$\chi\in\left\{V(\chi)\leq\min\left[\left(\frac{\varkappa_0}{(1-\Phi)c}\right)^{1/\alpha},\left(\frac{\varkappa_0}{(1-\Phi)\hat{c}}\right)^{1/\beta}\right]\right\}, \tag{82}$$

where the convergence is guaranteed for initial states within a sufficiently large compact set. Then, the settling time is

$$T\leq T_m=\frac{1}{c\Phi(\alpha-1)}+\frac{1}{\hat{c}\Phi(1-\beta)}. \tag{83}$$

Given the definition of V_n, we have

$$|y-y_d|\leq 2\left(\frac{\varkappa_0}{(1-\Phi)c}\right)^{1/2\alpha}. \tag{84}$$

The tracking error can be decreased within an ideal range in a fixed time by choosing the design parameters properly. □

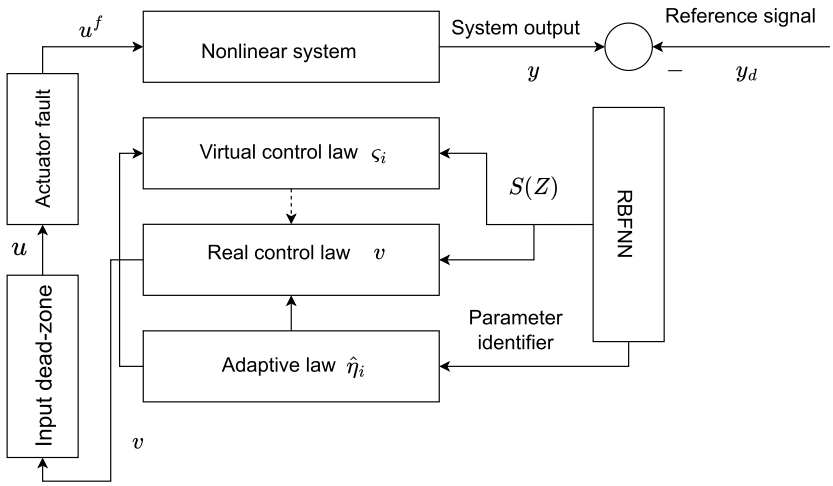

Fig. 2. Block diagram of the proposed adaptive fixed-time control design method.

Fig. 2 illustrates the proposed control scheme, providing a clearer understanding of the control procedures.

Remark 4. The convergence time bound T in (83) is independent of the initial conditions and ensures that the tracking error converges to a compact neighborhood of the origin within the fixed time T_m. Although the presence of bounded approximation errors and external disturbances prevents exact convergence to zero, the size of this neighborhood can be made arbitrarily small by appropriately tuning the controller parameters. Hence, the proposed adaptive fixed-time control scheme guarantees high-precision tracking performance within a predefined time bound, without imposing any restrictions on the initial states.

Remark 5. In practical systems, recovering to normal operation quickly after a fault is crucial. Existing finite-time control methods [36–38] face challenges as settling time depends on initial states, leading to longer recovery times. This paper proposes using two exponential terms in virtual control signals to establish an upper bound on settling time, independent of initial states. This approach ensures predictable and efficient recovery regardless of initial conditions.

Remark 6. The fixed-time performance of the proposed control system, while independent of the initial conditions, is influenced by the selection of design parameters such as k_i, q_i, ρ_i, $\bar{\rho}_i$, and a_i. Parameters k_i and q_i primarily determine the convergence rate, where higher values can accelerate convergence but may lead to larger control signal amplitudes, potentially causing actuator saturation. The parameters ρ_i and $\bar{\rho}_i$ affect robustness against disturbances and uncertainties, with larger values improving disturbance rejection at the cost of higher control effort. The parameter a_i shapes the convergence curve and indirectly impacts the fixed-time boundary; reducing a_i can decrease settling time but may induce high-frequency oscillations if chosen too small. Therefore, achieving satisfactory control performance requires careful tuning of these parameters. In practice, they are adjusted iteratively, typically through trial-and-error, to ensure a balance between fast fixed-time convergence, smooth control action, and practical feasibility of the control signals.

4. Simulation results

In this section, a simulation study along with a real-world example is provided to demonstrate the performance of the proposed control approach.

Example 1. Consider the following second-order nonlinear system as reported in [49]

$$\begin{cases} \dot{z} = -z - \chi_1^2 + 0.5, \\ \dot{\chi}_1 = (2 + \sin(\chi_1))\chi_2 + 0.1\sin(\chi_1\chi_2) + z\sin(\chi_1^2) \\ \dot{\chi}_2 = (2 + \cos(\chi_1\chi_2))u^f + 0.5\sin(\chi_1^2\chi_2^2) + \chi_1^2 z \\ y = \chi_1 \end{cases} \tag{85}$$

where χ_1 and χ_2 represent the state variables, u^f and y denote the input and output signals, $g_1 = 2 + \sin(\chi_1)$, $g_2 = 2 + \cos(\chi_1\chi_2)$, $f_1 = 0.1\sin(\chi_1\chi_2)$, $f_2 = 0.5\sin(\chi_1^2\chi_2^2)$, $\phi_1 = z\sin(\chi_1^2)$, $\phi_2 = \chi_1^2 z$.
The actuator faults model (2) is chosen as

$$u^f = \begin{cases} v & \text{if } t < 10 \\ (0.4 + 0.6\exp(-0.2t))u(v) + \chi_2\cos^2(\chi_1) & \text{if } t \geq 10 \end{cases} \tag{86}$$

where $K(t) = 0.4 + 0.6\exp(-0.2t)$ and $L(t) = \chi_2\cos^2(\chi_1)$.

The dead-zone model (3) is chosen as

$$u(v)=\begin{cases}(v(t)-0.5) & \text{if } v\geq 0.5\\ 0 & \text{if } -0.6<v(t)<0.5\\ 1.2(v(t)+0.6) & \text{if } v(t)\leq -0.6\end{cases} \tag{87}$$

where $m_r=1$, $m_l=1.2$, $b_r=0.5$ and $b_l=0.6$.
The objective is to develop an adaptive controller that guarantees the boundedness of all signals and ensures that the system output y follows the desired reference trajectory $y_d=0.5(\sin(t))$. To verify the validity of Assumption 6, consider choosing $V(z)=z^2$, then

$$\dot{V}(z)=2z(-z+\chi_1^2+0.5)\leq -2z^2+\frac{1}{4\epsilon}(2z)^2+\epsilon\chi_1^4+\frac{\epsilon}{4}+\frac{z^2}{\epsilon}. \tag{88}$$

By choosing $\epsilon=2.5$, we obtain

$$\dot{V}(z)\leq -1.2z^2+2.5\chi_1^4+0.625. \tag{89}$$

Furthermore, define $\theta_1(|z|)=0.5z^2$, $\theta_2(|z|)=2z^2$, $c_0=1.2$, $d=0.625$, and $\gamma(|\chi_1|)=2.5\chi_1^4$ to satisfy Assumption 6. Choose $\bar{a}=1\in(0,a_0)$ and define a dynamic signal r as

$$\dot{r}=-r+2.5\chi_1^4+0.625. \tag{90}$$

As per Theorem 1, the construction of the virtual control law ς_1, the real control law v, and the adaptive laws η_i is as follows

$$\varsigma_1=-k_1z_1^{2\alpha-1}-q_1z_1^{2\beta-1}-\frac{1}{2a_1^2}\hat{\eta}_1z_1P_1^T(X_1)P_1(X_1) \tag{91}$$

$$v=-k_2z_2^{2\alpha-1}-q_2z_2^{2\beta-1}-\frac{1}{2a_2^2}\hat{\eta}_2z_2P_2^T(X_2)P_2(X_2) \tag{92}$$

$$\dot{\hat{\eta}}_i=\frac{\kappa_i}{2a_i^2}z_i^2P_i^T(X_i)P_i(X_i)-\varrho_i\hat{\eta}_i-\bar{\varrho}_i\hat{\eta}_i,\quad i=1,2. \tag{93}$$

The control parameters are determined through a trial-and-error method as follows: $k_1=10$, $k_2=10$, $q_1=8$, $q_2=8$, $a_1=5$, $a_2=2$, $\kappa_1=2$, $\kappa_2=2$, $\varrho_1=2$, $\varrho_2=2$, $\bar{\varrho}_1=1$, $\bar{\varrho}_2=1$, and initial values are set at $\chi_1(0)=0.5$, $\chi_2(0)=0.5$, $\hat{\eta}_1(0)=0$, $\hat{\eta}_1(0)=0$, $z(0)=0$, $r(0)=0$. The basis vector functions $S_i(Z_i)$ (where $i=1,2$) are defined using a center of the receptive field $\mu_i=[-1.5,-1,-0.5,0,0.5,1,1.5]^T$ and Gaussian functions with a width $\tau=2$.

Fig. 3 presents the system output trajectory y along with the desired reference signal y_d. It can be seen that the output closely follows the reference, indicating that the proposed fixed-time adaptive controller achieves accurate tracking performance under various operating conditions. This demonstrates the controller's ability to compensate for uncertainties, actuator faults, input dead-zone, and external disturbances. In Fig. 4, the tracking error trajectory is shown, converging rapidly to a small neighborhood around zero. This confirms the fixed-time convergence property of the proposed method, which ensures that the error reaches a bounded region within a predefined time regardless of the initial conditions. Fig. 5 depicts the response of the state variable χ_2, illustrating the smooth and stable behavior of the system states under the proposed control strategy. Fig. 6 shows the estimated signals $\hat{\eta}_1$ and $\hat{\eta}_2$, reflecting the effectiveness of the radial basis function neural networks (RBFNNs) in approximating the unknown nonlinear functions and reducing the impact of unmodeled dynamics. Fig. 7 presents the control input v and the system input u^f, demonstrating that all control signals remain well-defined and bounded throughout the operation, which is critical for practical implementation. Fig. 8 illustrates the trajectories of z and the dynamic compensating signal r, highlighting the active mitigation of unmodeled dynamics and improvement in overall system robustness.
To further validate the performance of the proposed method, a comparative analysis is conducted with the finite-time adaptive control scheme reported in [36]. Fig. 9 shows the tracking errors obtained under both methods. It is observed that the proposed fixed-time controller achieves faster convergence of the tracking error, and the settling time remains independent of initial conditions. In contrast, the finite-time method exhibits convergence that varies with the initial states. Moreover, the steady-state error under the proposed approach is smaller, demonstrating superior tracking accuracy. This comparison highlights the advantages of the proposed fixed-time adaptive controller in terms of predictable settling time, enhanced robustness against disturbances and actuator nonlinearities, and improved transient performance over the finite-time approach. Overall, the figures collectively demonstrate that the proposed control scheme effectively ensures bounded closed-loop signals, achieves accurate tracking, mitigates unmodeled dynamics, and provides superior performance in comparison with existing methods.

To evaluate the effectiveness of the proposed fixed-time adaptive control method in comparison with the existing finite-time control approach [36], we employ the performance evaluation metrics described in [29]. These metrics provide quantitative measures to assess tracking accuracy, transient response, and robustness of the control schemes. The comparison between the proposed fixed-time control approach and the finite-time method [36] is conducted using the following metrics:

1. **Relative approximation error (RAE)**

$$\text{RAE}=\sqrt{\frac{\sum_{i=1}^{n}(y_i(t)-y_{id}(t))^2}{\sum_{i=1}^{n}(y_i(t))^2}} \tag{94}$$

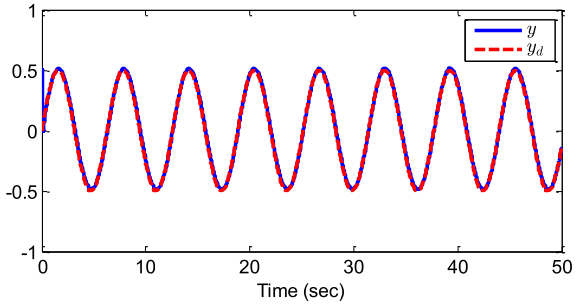

Fig. 3. Trajectories of system output y and reference signal y_d.

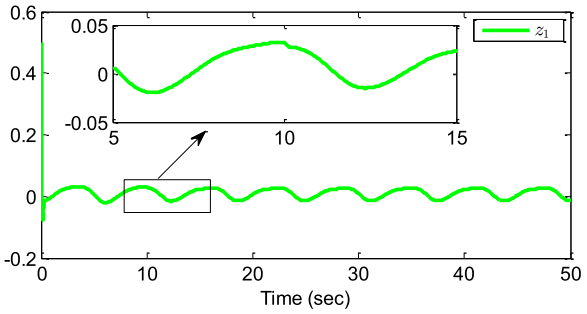

Fig. 4. Trajectory of tracking error z_1.

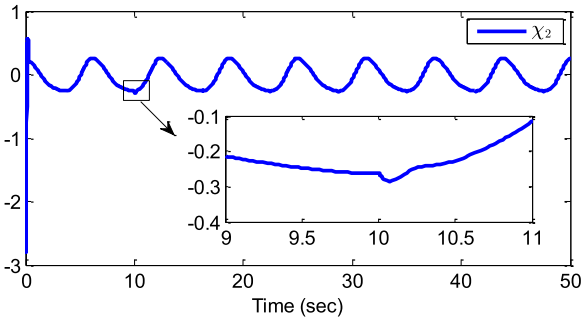

Fig. 5. Trajectory of state χ_2.

2. **Mean squared error (MSE)**

$$\text{MSE} = \frac{\sum_{i=1}^{n}(y_i(t) - y_{id}(t))^2}{n} \tag{95}$$

3. **Root mean squared error (RMSE)**

$$\text{RMSE} = \sqrt{\frac{\sum_{i=1}^{n}(y_i(t) - y_{id}(t))^2}{n}} \tag{96}$$

4. **Mean absolute error (MAE)**

$$\text{MAE} = \frac{1}{n}\sum_{i=1}^{n}|y_i(t) - y_{id}(t)| \tag{97}$$

where n represents the number of observations, y_i denotes the system's output, and y_{id} represents the desired reference signal.

The results presented in Table 1 demonstrate a clear performance improvement of the proposed fixed-time control method over the existing finite-time approach [36]. The evaluation metrics indicate that the proposed method achieves faster convergence, reduced tracking error, and improved transient response. These results highlight the effectiveness and robustness of the proposed control scheme in handling actuator faults, input dead-zone, and unmodeled dynamics, thereby validating its practical applicability and superiority over conventional finite-time approaches.

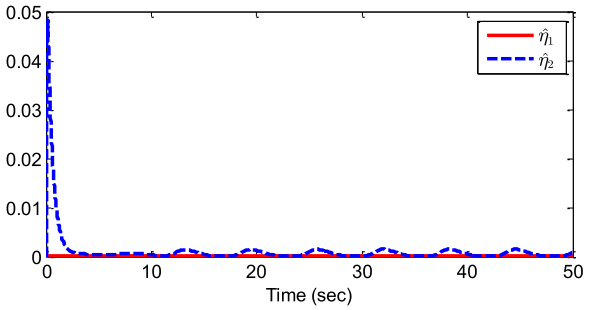

Fig. 6. Trajectories of adaptive laws $\hat{\eta}_1$ and $\hat{\eta}_2$.

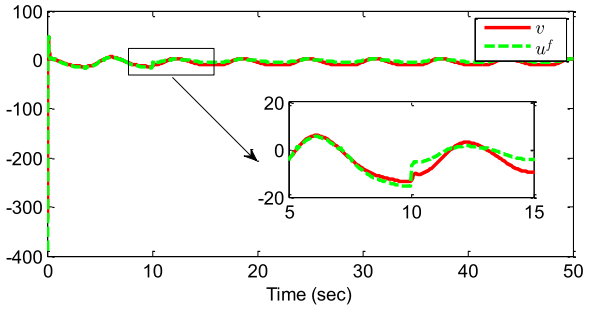

Fig. 7. Trajectories of control input v and system input u^f.

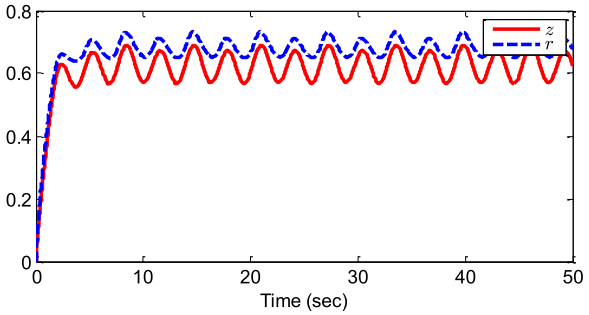

Fig. 8. Trajectories of z and r.

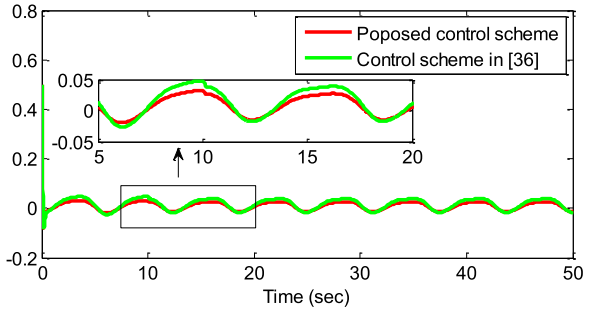

Fig. 9. Trajectory of tracking error z_1 under two methods.

Table 1
Comparison of the tracking performance using performance evaluation metrics.

Method	RAE	MSE	RMSE	MAE
Proposed method	0.1375	0.0027	0.0517	0.0209
Method in [36]	0.1597	0.0036	0.0600	0.0295

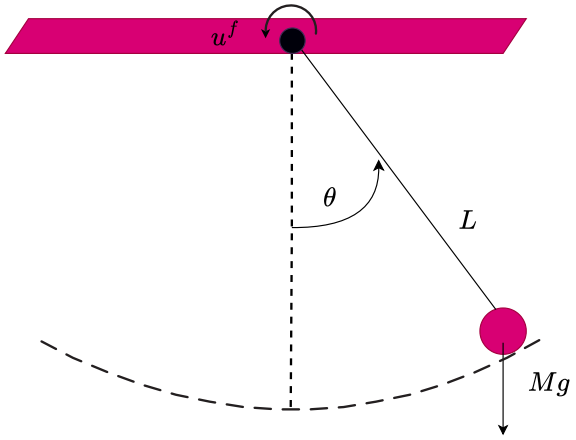

Fig. 10. Pendulum.

Example 2. To validate the proposed method further, a pendulum system depicted in Fig. 10 is utilized, and it can be described as follows [49]

$$ML\ddot{\theta} + BL\dot{\theta} + MgL\sin\theta = u, \tag{98}$$

where θ signifies the angle between the rod and the vertical upward direction, while $\dot{\theta}$ denotes the rod's angular velocity. The parameters M and L stand for the bob's mass and the rod's length, respectively. Additionally, B represents the frictional coefficient, and g indicates the acceleration due to gravity. For this particular system, the parameters are chosen as $M = 0.25$ kg, $L = 4$ m, $B = 0.25$, and $g = 10$ m/s^2.

By defining $\chi_1 = \theta$ and $\chi_2 = \dot{\theta}$, and taking into account the impact of unmodeled dynamics, actuator faults, dead-zone, and external disturbances, the pendulum system (98) can be rewritten as:

$$\begin{cases} \dot{z} = -2z + 0.25\chi_1^2 \\ \dot{\chi}_1 = x_2 + z\chi_1 + 0.2\sin(t) \\ \dot{\chi}_2 = \frac{1}{ML}u^f - \left(\frac{g}{L} + \frac{B}{M}\right)\sin(\chi_1\chi_2) + z\chi_2\sin(\chi_1) + 0.3\cos(t) \\ y = \chi_1 \end{cases} \tag{99}$$

where χ_1 and χ_2 represent the state variables, u^f and y denote the input and output signals, $g_1 = 1$, $g_2 = \frac{1}{ML}$, $f_1 = 0$, $f_2 = -\left(\frac{g}{L} + \frac{B}{M}\right)\sin(\chi_1\chi_2)$, $\phi_1 = z\chi_1$, $\phi_2 = z\chi_2\sin(\chi_1)$, $d_1 = 0.2\sin(t)$, $d_2 = 0.3\cos(t)$.
The actuator faults model (2) is chosen as

$$u^f = \begin{cases} v & \text{if } t < 5 \\ (0.4 + 0.6\exp(-0.2t))u(v) + \chi_2\cos^2(\chi_1) & \text{if } t \geq 5 \end{cases} \tag{100}$$

where $K(t) = 0.4 + 0.6\exp(-0.2t)$ and $L(t) = \chi_2\cos^2(\chi_1)$.
The dead-zone model (3) is chosen as

$$u(v) = \begin{cases} (v(t) - 0.5) & \text{if } v \geq 0.5 \\ 0 & \text{if } -0.6 < v(t) < 0.5 \\ 1.2(v(t) + 0.6) & \text{if } v(t) \leq -0.6 \end{cases} \tag{101}$$

where $m_r = 1$, $m_l = 1.2$, $b_r = 0.5$ and $b_l = 0.6$.
The goal is to create an adaptive neural controller that ensures the boundedness of all signals and enables the system output y to track the desired reference trajectory $y_d = \sin(0.5t)$. To verify the validity of Assumption 6, consider choosing $V(z) = z^2$, then

$$\dot{V}(z) = 2z(-z + 0.25\chi_1^2) \leq -2z^2 + \frac{1}{4\epsilon}(z)^2 + \epsilon\chi_1^4 + \frac{\epsilon}{4} + \frac{z^2}{\epsilon}. \tag{102}$$

By choosing $\epsilon = 2.5$, we obtain

$$\dot{V}(z) \leq -1.5z^2 + 2.5\chi_1^4 + 0.625. \tag{103}$$

Furthermore, define $\theta_1(|z|) = 0.5z^2$, $\theta_2(|z|) = 2z^2$, $c_0 = 1.5$, $d = 0.625$, and $\gamma(|\chi_1|) = 2.5\chi_1^4$ to satisfy Assumption 6. Choose $\bar{a} = 1 \in (0, a_0)$ and define a dynamic signal r as

$$\dot{r} = -r + 2.5\chi_1^4 + 0.625. \tag{104}$$

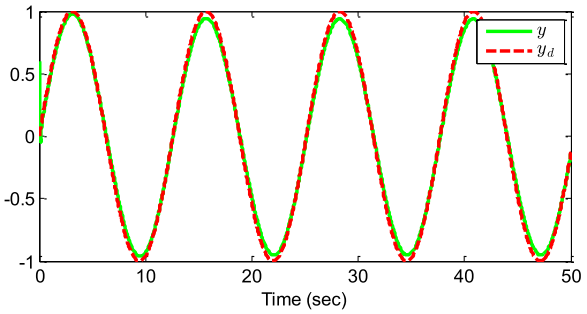

Fig. 11. Trajectories of system output y and reference signal y_d.

Table 2
Comparison of the tracking performance using performance evaluation metrics.

Method	RAE	MSE	RMSE	MAE
Proposed method	0.1157	0.0066	0.0810	0.0477
Method in [36]	0.1422	0.0092	0.0960	0.0636

As per Theorem 1, the construction of the virtual control law ς_1, the real control law υ, and the adaptive laws η_i is as follows

$$\varsigma_1 = -k_1 z_1^{2\alpha-1} - q_1 z_1^{2\beta-1} - \frac{1}{2a_1^2}\hat{\eta}_1 z_1 P_1^T(X_1)P_1(X_1) \tag{105}$$

$$\upsilon = -k_2 z_2^{2\alpha-1} - q_2 z_2^{2\beta-1} - \frac{1}{2a_2^2}\hat{\eta}_2 z_2 P_2^T(X_2)P_2(X_2) \tag{106}$$

$$\dot{\hat{\eta}}_i = \frac{\kappa_i}{2a_i^2} z_i^2 P_i^T(X_i)P_i(X_i) - \varrho_i\hat{\eta}_i - \bar{\varrho}_i\hat{\eta}_i, \quad i = 1, 2. \tag{107}$$

The control parameters are determined through a trial-and-error method as $k_1 = 25$, $k_2 = 25$, $q_1 = 20$, $q_2 = 20$, $a_1 = 5$, $a_2 = 2$, $\kappa_1 = 2$, $\kappa_2 = 2$, $\varrho_1 = 1$, $\varrho_2 = 1$, $\bar{\varrho}_1 = 2$, $\bar{\varrho}_2 = 1$. Initial values are set at $\chi_1(0) = 0.6$, $\chi_2(0) = 0.1$, $\hat{\eta}_1(0) = 0$, $\hat{\eta}_2(0) = 0$, $z(0) = 0$, $r(0) = 0$. The basis vector functions $S_i(Z_i)$, where $i = 1, 2$, are determined using a center of the receptive field $\mu_i = [-1.5, -1, -0.5, 0, 0.5, 1, 1.5]^T$ and Gaussian functions with a width $\tau = 2$.

Fig. 11 illustrates the trajectories of the system output y and the reference signal y_d. It is observed that the output signal closely follows the desired reference, demonstrating the accurate tracking capability of the proposed fixed-time adaptive controller. This shows that the controller effectively compensates for uncertainties, actuator faults, input dead-zone, and external disturbances. In Fig. 12, the tracking error trajectory is presented, showing rapid convergence to a small neighborhood around zero. This confirms the fixed-time convergence property of the proposed controller and indicates that the system achieves the desired performance within a predictable and predefined time, independent of the initial conditions. Fig. 13 depicts the response of the state variable χ_2, highlighting the smooth and stable behavior of the system states under the proposed control strategy. Fig. 14 shows the estimated signals $\hat{\eta}_1$ and $\hat{\eta}_2$, which demonstrate the effectiveness of the radial basis function neural networks (RBFNNs) in approximating unknown nonlinear functions. This ensures that the influence of unmodeled dynamics is mitigated, contributing to the overall robustness and performance of the system. Fig. 15 presents the control input υ and the system input u^f, showing that both signals remain bounded and well-defined throughout the operation. This is particularly important for practical implementation, as it guarantees that the actuators operate within safe limits even in the presence of faults and uncertainties. Fig. 16 illustrates the trajectories of z and the dynamic compensating signal r, which actively reduces the effect of unmodeled dynamics, ensuring that the system maintains stability and desired tracking performance under uncertain conditions.

To further validate the effectiveness of the proposed method, a comparison is conducted with the finite-time adaptive control scheme reported in [36]. Fig. 17 shows the tracking errors obtained under both methods. It can be observed that the proposed fixed-time method achieves faster convergence and reduced steady-state error compared to the finite-time approach. In addition, the settling time with the proposed method remains independent of the initial states, whereas the finite-time scheme exhibits convergence that depends on the initial conditions. This highlights the practical advantage of the proposed approach in achieving predictable transient performance. The comparison also demonstrates improved robustness and reliability in the presence of actuator faults, input dead-zone, and unmodeled dynamics, confirming that the proposed fixed-time adaptive control strategy provides superior overall performance relative to the conventional finite-time approach.

The same performance evaluation metrics used in Example 1 are applied in this example as well. Table 2 distinctly showcases the advantage of the proposed fixed-time control method compared to the existing finite-time control method [36]. This underscores the effectiveness of our approach, as highlighted by the performance evaluation metrics.

Table 2 presents a quantitative comparison of the proposed fixed-time control method with the existing finite-time approach [36] using performance evaluation metrics. The results indicate that the proposed method achieves slightly better performance in terms

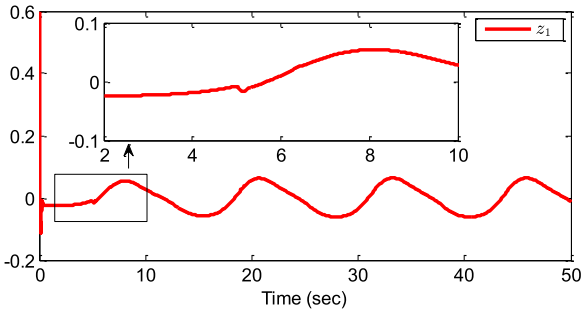

Fig. 12. Trajectory of tracking error z_1.

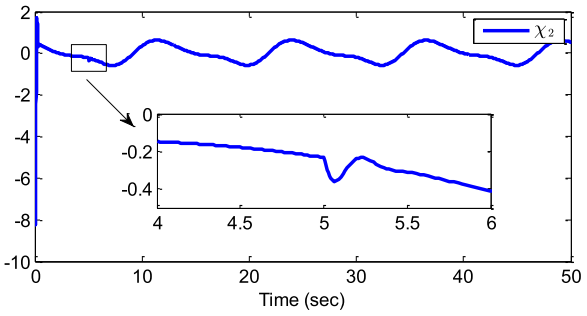

Fig. 13. Trajectory of state χ_2.

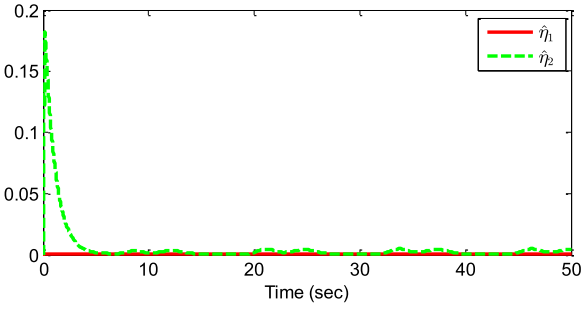

Fig. 14. Trajectories of adaptive laws $\hat{\eta}_1$ and $\hat{\eta}_2$.

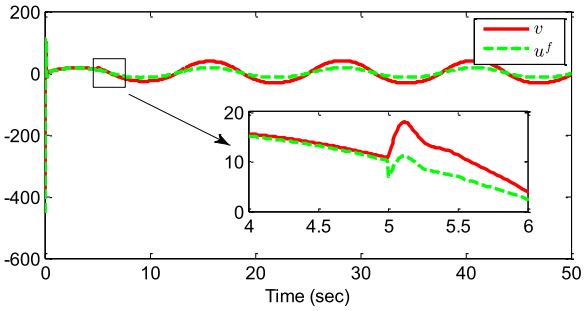

Fig. 15. Trajectories of control input v and system input u^f.

of faster convergence, smaller tracking errors, and improved transient response. These improvements highlight the effectiveness of the proposed control strategy in handling actuator faults, input dead-zone, external disturbances, and unmodeled dynamics. The comparison demonstrates that the proposed fixed-time controller not only ensures predictable settling time independent of initial conditions but also enhances robustness and reliability compared to the conventional finite-time method.

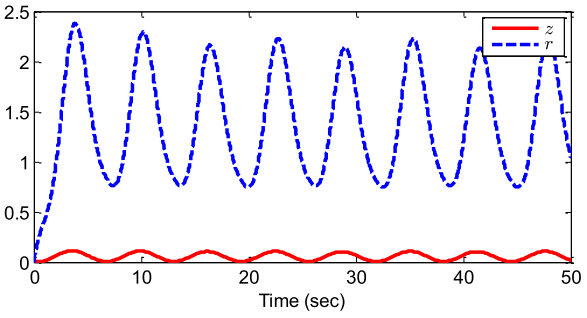

Fig. 16. Trajectories of z and r.

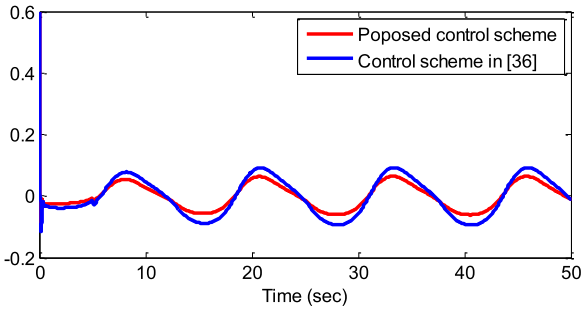

Fig. 17. Trajectory of tracking error z_1 under two methods.

Remark 7. Examples 1 and 2 are taken from the existing study [49]. Compared to [49], this paper considers unmodeled dynamics, actuator faults, dead-zone, and external disturbances in nonlinear systems, making it more challenging and relevant from a practical perspective.

5. Conclusion

This research addresses the adaptive fixed-time control problem for nonstrict-feedback nonlinear systems, specifically tackling challenges such as actuator faults, input dead-zone, external disturbances, and unmodeled dynamics. Radial basis function neural networks are employed to approximate unknown nonlinear functions, and a dynamic compensating signal is incorporated to mitigate the influence of unmodeled dynamics. By combining Lyapunov stability theory with the backstepping approach, the proposed adaptive fixed-time controller ensures boundedness of all closed-loop signals and achieves the desired tracking performance within a fixed time. Importantly, the settling time is independent of initial conditions and is determined solely by the selected design parameters. Two illustrative examples demonstrate the effectiveness of the proposed approach.

While the proposed method provides robust and efficient control, certain limitations remain. The current design focuses on continuous-time nonstrict-feedback systems and may require adaptation for discrete-time or higher-order nonlinear systems. The controller assumes that bounds of actuator faults and unmodeled dynamics are known or estimable, which may not always be feasible in practice. Additionally, the computational complexity increases with system order and the number of approximated nonlinear functions. Addressing these limitations, such as extending the approach to discrete-time or stochastic systems, handling completely unknown fault bounds, or improving computational efficiency, represents potential avenues to further enhance the applicability and performance of the proposed control strategy.

CRediT authorship contribution statement

Mohamed Kharrat: Writing – review & editing, Writing – original draft, Visualization, Validation, Software, Resources, Methodology, Investigation, Formal analysis, Data curation, Conceptualization; **Paolo Mercorelli:** Writing – review & editing, Writing – original draft, Visualization, Validation, Supervision, Resources, Project administration, Methodology, Investigation, Funding acquisition, Formal analysis, Data curation, Conceptualization.

Data availability

All data generated or analysed during this study are included in this published article.

Declaration of competing interest

The authors declare that they have no known competing financial interests or personal relationships that could have appeared to influence the work reported in this paper.

References

[1] Li Y, Tong S. Finite-time adaptive backstepping control for uncertain nonlinear strict-feedback systems with full state triggering. Automatica 2024;163:111574.
[2] Xu Z, Zhou X, Dong Z, Hu X, Sun C, Shen H. Observer-based prescribed performance adaptive neural output feedback control for full-state-constrained nonlinear systems with input saturation. Chaos Solitons Fractals 2023;173:113593.
[3] Ning P-J, Hua C-C, Li K, Meng R. Event-triggered adaptive prescribed-time control for nonlinear systems with uncertain time-varying parameters. Automatica 2023;157:111229.
[4] Zhao X, Wang X, Zhang S, Zong G. Adaptive neural backstepping control design for a class of nonsmooth nonlinear systems. IEEE Trans Syst Man Cybern Syst 2018;49:1820–31. https://doi.org/10.1109/TSMC.2018.2823381
[5] Zhou J, Wen C, Wang W, Yang F. Adaptive backstepping control of nonlinear uncertain systems with quantized states. IEEE Trans Automat Control 2019;64:4756–63.
[6] Zhang T, Zhang W. Adaptive practical prescribed-time control for uncertain nonlinear systems with time-varying parameters. Chaos Solitons Fractals 2024;189:115677.
[7] Kharrat M, Krichen M, Alkhalifa L, Gasmi K. Neural networks-based adaptive command filter control for nonlinear systems with unknown backlash-like hysteresis and its application to single link robot manipulator. AIMS Math 2024;9:959–73.
[8] Li Y, Shao X, Tong S. Adaptive fuzzy prescribed performance control of nontriangular structure nonlinear systems. IEEE Trans Fuzzy Syst 2019;28:2416–26.
[9] Sui S, Yu Y, Tong S, Chen CP. Event-triggered robust fuzzy adaptive control for non-strict feedback nonlinear systems with prescribed performance. Appl Math Comput 2024;474:128701.
[10] Zhang L, Deng C, Che W-W, An L. Adaptive backstepping control for nonlinear interconnected systems with prespecified-performance-driven output triggering. Automatica 2023;154:111063.
[11] Xia Y, Xiao K, Geng Z. Event-based adaptive fuzzy control for stochastic nonlinear systems with prescribed performance. Chaos Solitons Fractals 2024;180:114501.
[12] Shanmugam L, Joo YH. Adaptive neural networks-based integral sliding mode control for ts fuzzy model of delayed nonlinear systems. Appl Math Comput 2023;450:127983.
[13] Li Y, Tong S. Adaptive fuzzy output constrained control design for multi-input multi-output stochastic nonstrict-feedback nonlinear systems. IEEE Trans Cybern 2016;47:4086–95.
[14] Wang W, Li Y, Tong S. Neural network-based adaptive event-triggered consensus control of nonstrict-feedback nonlinear systems. IEEE Trans Neural Netw Learn Syst 2020;32:1750–64.
[15] Cao B, Nie X. Event-triggered adaptive neural networks control for fractional-order nonstrict-feedback nonlinear systems with unmodeled dynamics and input saturation. Neural Netw 2021;142:288–302.
[16] Wang H, Liu PX, Xie X, Liu X, Hayat T, Alsaadi FE. Adaptive fuzzy asymptotical tracking control of nonlinear systems with unmodeled dynamics and quantized actuator. Inf Sci 2021;575:779–92.
[17] Shi X, Lim CC, Xu S, Shi P. Robust approximation-based adaptive control of multiple state delayed nonlinear systems with unmodeled dynamics. Int J Robust Nonlinear Control 2018;28:3303–23.
[18] Dogan KM, Gruenwald BC, Yucelen T, Muse JA. Relaxing the stability limit of adaptive control systems in the presence of unmodeled dynamics. Int J Control 2018;91:1774–84.
[19] Bi W, Wang T. Adaptive fuzzy decentralized control for nonstrict-feedback nonlinear systems with unmodeled dynamics. IEEE Trans Syst Man Cybern Syst 2020;52:275–86.
[20] Tong S, Li Y. Observer-based fuzzy adaptive robust control of nonlinear systems with time delays and unmodeled dynamics. Neurocomputing 2010;74(1–3):369–78.
[21] Yin S, Shi P, Yang H. Adaptive fuzzy control of strict-feedback nonlinear time-delay systems with unmodeled dynamics. IEEE Trans Cybern 2015;46:1926–38.
[22] Kharrat M, Krichen M, Alkhalifa L, Gasmi K. Neural-networks-based adaptive fault-tolerant control of nonlinear systems with actuator faults and input quantization. IEEE Access 2023;11:137680–7.
[23] Kharrat M. Neural networks-based adaptive fault-tolerant control for stochastic nonlinear systems with unknown backlash-like hysteresis and actuator faults. J Appl Math Comput 2024;70:1995–2018.
[24] Wu L-B, He X-Q, Guo L-D, Huang S-J, Hu Y-H. Neural network adaptive switched fault-tolerant control of uncertain nonlinear systems with full state constraints. Neurocomputing 2024;598:128034.
[25] Yang H, Yin S, Kaynak O. Neural network-based adaptive fault-tolerant control for markovian jump systems with nonlinearity and actuator faults. IEEE Trans Syst Man Cybern Syst 2020;51:3687–98.
[26] Li YX, Yang GH. Fuzzy adaptive output feedback fault-tolerant tracking control of a class of uncertain nonlinear systems with nonaffine nonlinear faults. IEEE Trans Fuzzy Syst 2015;24:223–34.
[27] Deng X, Zhang C, Ge Y. Adaptive neural network dynamic surface control of uncertain strict-feedback nonlinear systems with unknown control direction and unknown actuator fault. J Franklin Inst 2022;359:4054–73.
[28] Ma L, Xu N, Zhao X, Zong G, Huo X. Small-gain technique-based adaptive neural output-feedback fault-tolerant control of switched nonlinear systems with unmodeled dynamics. IEEE Trans Syst Man Cybern Syst 2020;51(11):7051–62. https://doi.org/10.1109/TSMC.2020.3001578
[29] Alruwaily Y, Kharrat M. Funnel-based adaptive neural fault-tolerant control for nonlinear systems with dead-zone and actuator faults: application to rigid robot manipulator and inverted pendulum systems. Complexity 2024;2024:5344619.
[30] Li H, Bai L, Wang L, Zhou Q, Wang H. Adaptive neural control of uncertain nonstrict-feedback stochastic nonlinear systems with output constraint and unknown dead zone. IEEE Trans Syst Man Cybern Syst 2016;47(8):2048–59.
[31] Ma L, Huo X, Zhao X, Zong GD. Observer-based adaptive neural tracking control for output-constrained switched mimo nonstrict-feedback nonlinear systems with unknown dead zone. Nonlinear Dyn 2020;99(2):1019–36.
[32] Shi X, Lim CC, Shi P, Xu S. Adaptive neural dynamic surface control for nonstrict-feedback systems with output dead zone; vol. 29. IEEE; 2018. https://doi.org/10.1109/TNNLS.2018.2791714
[33] Su X, Liu Z, Lai G. Event-triggered robust adaptive control for uncertain nonlinear systems preceded by actuator dead-zone. Nonlinear Dyn 2018;93(1):219–31.
[34] Lan J, Liu YJ, Liu L, Tong S. Adaptive output feedback tracking control for a class of nonlinear time-varying state constrained systems with fuzzy dead-zone input. IEEE Trans Fuzzy Syst 2020;29(8):1841–52.
[35] Yang W, Pan Y, Liang H. Observer-based adaptive neural network control for uncertain nonlinear systems with prescribed performance and fuzzy dead-zone input. Circuits Syst Signal Process 2021;40(2):572–97.
[36] Sun Y, Chen B, Lin C, Wang H. Finite-time adaptive control for a class of nonlinear systems with nonstrict feedback structure. IEEE Trans Cybern 2017;48(8):2774–82.
[37] Li M, Zhang J, Li S, Wu F. Adaptive finite-time fault-tolerant control for the full-state-constrained robotic manipulator with novel given performance. Eng Appl Artif Intell 2023;125:106650.
[38] Wang H, Meng Z, Ma J, Zhao X. Adaptive fixed-time dynamic surface tracking control for high-order nonstrict-feedback nonlinear switched systems. Neurocomputing 2024;589:127590.

[39] Xu K, Wang H, Liu PX. Adaptive fuzzy finite-time tracking control of nonlinear systems with unmodeled dynamics. Appl Math Comput 2023;450:127992.
[40] Wang F, Liu Z, Zhang Y, Chen CP. Adaptive finite-time control of stochastic nonlinear systems with actuator failures. Fuzzy Sets Syst 2019;374:170–83.
[41] Ding L, Li S, Gao H, Liu YJ, Huang L, Deng Z. Adaptive neural network-based finite-time online optimal tracking control of the nonlinear system with dead zone. IEEE Trans Cybern 2019;51(5):382–92.
[42] Ni J, Wu Z, Liu L, Liu C. Fixed-time adaptive neural network control for nonstrict-feedback nonlinear systems with dead zone and output constraint. ISA Trans 2020;97:458–73.
[43] Song X, Sun P, Song S, Stojanovic V. Event-driven neural network adaptive fixed-time control for nonlinear systems with guaranteed performance. J Franklin Inst 2022;359(9):4138–59.
[44] Ba D, Li YX, Tong S. Fixed-time adaptive neural tracking control for a class of uncertain nonstrict nonlinear systems. Neurocomputing 2019;363:273–80.
[45] Yang W, Pan Y, Liang H. Event-triggered adaptive fixed-time neural network control for constrained nonstrict-feedback nonlinear systems with prescribed performance. Neurocomputing 2021;422:332–44.
[46] Liang Y, Li YX, Hou Z. Adaptive fixed-time tracking control for stochastic pure-feedback nonlinear systems. Int J Adapt Control Signal Process 2021;35(9):1712–31.
[47] Sun Y, Zhang L. Fixed-time adaptive fuzzy control for uncertain strict feedback switched systems. Inf Sci 2021;546:742–52.
[48] Wang H, Shen L. Adaptive fuzzy fixed-time tracking control for nonlinear systems with time-varying full-state constraints and actuator hysteresis. IEEE Trans Fuzzy Syst 2022;31(7):1352–61.
[49] Wang H, Xu K, Qiu J. Event-triggered adaptive fuzzy fixed-time tracking control for a class of nonstrict-feedback nonlinear systems. IEEE Trans Circuits Syst I 2021;68(7):3058–68.